

Study on CO₂ Corrosion in Oil Producing Well

by

Mohd Noor Hazman bin Mansor

Dissertation submitted in partial fulfilment of
the requirements for the
Bachelor of Engineering (Hons)
(Mechanical Engineering)

JANUARY 2009

Universiti Teknologi PETRONAS

Bandar Seri Iskandar

31750 Tronoh

Perak Darul Ridzuan

t
TU
871 5
m 607
2009

1) Oil field - Equipment and supplies - corrosion
2) Corrosion and oil - corrosive
3) Thesis

CERTIFICATION OF APPROVAL

Study on CO₂ Corrosion in Oil Producing Well

by

Mohd Noor Hazman bin Mansor

A project dissertation submitted to the
Mechanical Engineering Programme
Universiti Teknologi PETRONAS
in partial fulfilment of the requirement for the
BACHELOR OF ENGINEERING (Hons)
(MECHANICAL ENGINEERING)

Approved by,



Assoc. Prof. Dr. Razali Hamzah

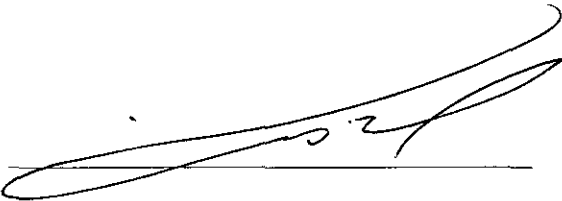
UNIVERSITI TEKNOLOGI PETRONAS

TRONOH, PERAK

January 2009

CERTIFICATION OF ORIGINALITY

This is to certify that I am responsible for the work submitted in this project, that the original work is my own except as specified in the references and acknowledgements, and that the original work contained herein have not been undertaken or done by unspecified sources or persons.



MOHD NOOR HAZMAN BIN MANSOR

ABSTRACT

The purpose of this project is to study the CO₂ corrosion in oil production wells and the focus of the study will be on the tubing component of the production string. The main objectives of the project are; a) To study the material used in a well production string. b) To determine the average CO₂ corrosion rate of a typical well production string. As for the problem statement of this project, in oil and gas industry, CO₂ corrosion has been a recognized problem in production and transportation facilities for many years e.g. in the tubing string of an oil producing well. The corroded tubing will cause leakage and tubing failure hence, disrupt oil production. The scopes of study for this project consist of identifying the rate of CO₂ corrosion during the production life time of the tubing string and determine the factors leading to the CO₂ corrosion. In order to provide a reliable prediction on the behavior of CO₂ corrosion on tubing steel, the project's methodology used Weight Loss Method using Autoclave Machine and Linear Polarization Resistance Method (LPR) to simulate the actual environment in the tubing during the oil production and analyze the CO₂ corrosion rate. The laboratory experiments are conducted on API L 80 type steel. The Weighted Loss Method is conducted in stagnant condition using 3 wt% NaCl over a series of parameters which includes pressure = 10 bar, 40 bar and 60 bar, pH=5 and temperature at 25 °C. The LPR method is conducted in flowing solution using 3 wt% NaCl over a series of parameters which includes temperature = 25 °C, 40 °C and 60 °C, pH = 5 and pressure at 1 atm. All data were collected and analyzed using Weighted Loss Method, LPR, SEM, OM and Hardness (Vicker) Test to determine the CO₂ corrosion rate and the effects on the L 80 steel. As for the findings, the average CO₂ corrosion rates in API L 80 steel yield from the laboratory test ranges from 1.3 mm/yr to 4.7 mm/yr.

Keywords

CO₂ corrosion rate, FeCO₃ film layers, Weighted Loss Method, LPR Method, API L-80 steel, SEM, Vicker Test

ACKNOWLEDGEMENTS

My highest gratitude to our Allah S.W.T. for all the blessings He has showered onto us.

Thank you to my supervisors, AP Dr. Razali Hamzah for the tremendous support, advice, guidance and encouragement throughout this project and in the preparation of this report, postgraduate students; Mr. Yuli Panca Asmara, Mr. Budi Agung Kurniawan, and Ms. Anis Amilah Ab Rahman for their priceless advice and mentoring throughout this project, PETRONAS Carigali Sdn. Bhd. engineer; Ms Suzanna Juyanty , fellow colleagues, and technicians of UTP Mechanical Laboratory for guiding me throughout the whole process of completing this project.

My deepest appreciation to my family - my parents, Mr. Mansor Hashim and Mrs. Haspiah Sulor, and my siblings, individuals especially Ms. Nurul Ashikin Tasnuddin Abu Bakar and Mr. Ameirul Azraie Mustadza for assisting me and giving me the support I needed.

TABLE OF CONTENTS

CERTIFICATION OF APPROVAL	i
CERIFICATION OF ORIGINALITY	ii
ABSTRACT	iii
ACKNOWLEDGEMENTS	iv
LIST OF FIGURES	vii
LIST OF TABLES	ix
CHAPTER 1: INTRODUCTION	1
1.1 Background of Study	1
1.2 Problem Statement	2
1.3 Objectives	2
1.4 Scope of Study	3
1.5 Relevancy of the Project	3
1.6 Feasibility of the Project	4
CHAPTER 2: LITERATURE REVIEW	4
2.1 Types of Oil Producing Well	4
2.2 Components of a Typical Oil Producing Well	6
2.3 Particles Flow in Oil Producing Well	11
2.4 Basic of CO ₂ Corrosion	14
2.5 Tests for CO ₂ Corrosion	18
CHAPTER 3: METHODOLOGY	22
3.1 Overall Project Flowchart	22
3.2 Weighted Loss Method using Autoclave	23
3.3 Linear Polarization Resistance Method	27
3.4 Scanning Electron Microscopic	31

3.5	Optical Microscopic Test	32
3.6	Microhardness (Vicker) Test	32
CHAPTER 4:	RESULTS AND DISCUSSION	33
4.1	Actual Data from Tukau 45L Oil Producing Well	33
4.2	Weighted Loss Method using Autoclave Test Results	35
4.3	Linear Polarization Resistance Method Test Results	37
4.4	Scanning Electron Microscopic Test Results		38
4.5	Optical Microscopic Test Results	41
4.6	Microhardness (Vicker) Test Results	42
CHAPTER 5:	CONCLUSION AND RECOMMENDATIONS		44
5.1	Conclusion	44
5.2	Recommendations	45
REFERENCES	46
APPENDICES	48

LIST OF FIGURES

Figure 2.1: Directional/ Vertical Well	5
Figure 2.2: Deviated Well	5
Figure 2.3: Horizontal and Multilateral Well	6
Figure 2.4: Cased, Cemented and Perforated Completion	7
Figure 2.5: API L-80 steel	10
Figure 2.6: Types of Corrosion in Oil Producing Well.	13
Figure 2.7: Autoclave Corrosion Test Equipment.	19
Figure 3.1: L-80 Steel Specimen for Weighted Loss Method using Autoclave	24
Figure 3.2: Schematic Diagram for Weighted Loss Method using Autoclave	25
Figure 3.3: Real Weighted Loss Method using Autoclave Test Setup	25
Figure 3.4: Working Electrode used in the LPR Test	28
Figure 3.5: Schematic Diagram of LPR Test	29
Figure 3.6: Real LPR Test Setup in Laboratory	30
Figure 3.7: SEM Machine	32
Figure 4.1: Depth vs. Pressure Graph for Tukau 45L Well	35
Figure 4.2: Temperature vs. Depth Graph for Tukau 45L Well	35
Figure 4.3: Average CO ₂ Corrosion Rates from LPR Test at Different Rotational Rates and Different Temperature	38
Figure 4.4: Typical CO ₂ Corrosion Rates in Aqueous Solution	40

Figure 4.5: SEM micrographs of L-80 steel that not-affected with any electrochemical reaction. (a) 100x (b) 500x (c) 1000x	41
Figure 4.6: L-80 steel specimen at 48 hours immersion in 3% NaCl solution pH 5, at pressure of 10 bar and temperature 25 °C (a) 100x (b) 500x (c) 1000x	43
Figure 4.7: L-80 steel specimen at 48 hours immersion in 3% NaCl solution pH 5, at pressure of 40 bar and temperature 25 °C (a) 100x (b) 500x (c) 1000x	44
Figure 4.8: L-80 steel specimen at 48 hours immersion in 3% NaCl solution pH 5, at pressure of 60 bar and temperature 25 °C (a) 100x (b) 500x (c) 1000x	45
Figure 4.9: OM micrographs of L-80 steel that not-affected with any electrochemical reaction	46
Figure 4.10: L-80 steel specimen at 48 hours immersion in 3% NaCl solution pH 5, at pressure of 10 bar and temperature 25 °C	47
Figure 4.11: L-80 steel specimen at 48 hours immersion in 3% NaCl solution pH 5, at pressure of 40 bar and temperature 25 °C	47
Figure 4.12: L-80 steel specimen at 48 hours immersion in 3% NaCl solution pH 5, at pressure of 60 bar and temperature 25 °C	48

LIST OF TABLES

Table 2.1: Casing Intervals	8
Table 2.2: Chemical composition of API L-80 steel.	10
Table 3.1: The constant values to calculate the corrosion rate in various units	23
Table 3.2: Chemical Composition of API L-80 Specimen	24
Table 4.1: Data Acquired from FGS Operation in Tukau 45L Well	34
Table 4.2: Average Weight Differences in API L-80 Steel Specimens	36
Table 4.3: Average CO ₂ Corrosion Rates in API L-80 Steel from Weighted Loss Method Test	37
Table 4.4: Average CO ₂ Corrosion Rates in API L-80 Steel from LPR Test	38
Table 4.5: Average Hardness of L-80 Steel Specimens	49

CHAPTER 1

INTRODUCTION

1.1 Background of Study

Corrosion is the degradation of the material due to chemical reaction with the environment. Corrosion problem is becoming an increasing threat to the integrity of oil field structures including pipelines, casing and tubing [1]. It is a serious problem in oil and gas industry all over the world. Most of the oil field structures encountered the corrosion problem because most of the equipments are made from steel and the natural existence of corroding agents to initiate the chemical reaction. Although high cost corrosion resistance alloys (CRAs) were developed to be able to resist the corrosion, steel is still the most cost effective material used in oil and gas facilities and structures [3]. The concern on the high cost remedial process for corrosion problematic well leads to the initiation of this project.

The tubing string is the most frequent component in a production well that will be corroded. The presence of CO₂ in produced fluids can result in very high corrosion rate particularly where the mode of attack on the tubing steel is localized. An aqueous phase is normally associated with the oil and gas being produced by the well [1]. The inherent corrosivity of this aqueous phase is dependent on the concentration of dissolved acidic gases and the water chemistry. The presences of CO₂ with the combination of water make the production potentially very corrosive.

CO₂ corrosion rate is dependent on the environmental effects such as temperature, pressure, pH, CO₂ partial pressure, flow velocity, CO₂ concentration and the formation of FeCO₃ layers [8]. The analysis of CO₂ corrosion rates have been carried out extensively to provide a reliable prediction on the behavior of CO₂ corrosion and leads to cost-effective and safe design of facilities used in the oil and gas industry.

In order to predict the behavior of CO₂ corrosion, Weight Loss Method and Linear Polarization Resistance Method (LPR) will be used to analyze both CO₂ corrosion rate and the effects on the tubing steel.

1.2 Problem Statement

Study on CO₂ corrosion has been carried out extensively for many years to observe the behavior of CO₂ corrosion on the steel in production facilities used in the oil and gas industry. The main reason in conducting the study and analysis is to gain understanding on CO₂ corrosion rate in the tubing component of oil producing string.

1.2.1 Problem Identification

Most of the studies on CO₂ corrosion rate were focused in the pipeline and platform materials such as API X-52, X-56, X-60, X-65 and N-80 steel. The study on CO₂ corrosion in the production tubing steel, API L-80 steel is crucial as the production fluid from the reservoir contains numerous amount of CO₂ gas which is typically 5% to 10% v/v in Malaysia's oilfields. Most of the oil producing wells in Malaysia are gas lifted wells and produced high in gas-oil-ratio (GOR). However, the concentration of CO₂ gas is different in different oil producing well. In gas lifted well, CO₂ gas is pumped into the production well to enhance the oil production and caused high concentration of CO₂ gas in the well.

1.2.2 Significance of the Project

The aim of this project was to study and analyze CO₂ corrosion effects and CO₂ corrosion rate using Weight Loss Method and LPR Method. It is important to understand the behavior of CO₂ corrosion in API L-80 steel and the ranges of CO₂ corrosion rate to minimize the CO₂ corrosion failure in oil producing string and lead to cost-effective and safe design of production facilities used in the oil and gas industry.

1.3 Objectives

The objectives of this project were:

- a. To study the material used in the well production string
- b. To determine the average CO₂ corrosion rate of a typical well production string

1.4 Scope of Study

The scopes of study of this project were:

- a. To conduct the CO₂ corrosion test on API L-80 steel using Weight Loss Method and Linear Polarization Resistance Method.
- b. To study and analyze the effect CO₂ corrosion on API L-80 steel using Scanning Electronic Microscopy (SEM) and Optical Microscope (OM) test.

1.5 Relevancy of the Project

The study of CO₂ corrosion in oil producing well is important especially in oil and gas industry. The results obtained from the laboratory tests will help to provide better understanding on the behavior of CO₂ corrosion. A thorough understanding on the effects of CO₂ corrosion and CO₂ corrosion rate in API L-80 will provide useful information thus help in providing reliable prediction of CO₂ corrosion which leads to cost-effective and safe design of production tubing used in the oil producing well.

1.6 Feasibility of the Project

The project was started by collecting reading materials such as books, journals and technical papers specifically on oil producing string components, CO₂ corrosion of steel, Weight Loss Method using Autoclave manual and LPR technique. Research was done continuously throughout this project to get a better understanding. The project was then focused on conducting laboratory experiments on API L-80 steel in CO₂ environment whereby analysis were carried out using Weight Loss Method, LPR and other techniques such as SEM, OM and Hardness (Vicker) Testing to determine the CO₂ corrosion rate and effects.

CHAPTER 2

LITERATURE REVIEW

In order to gain better understanding in the CO₂ corrosion phenomena that may occurred in oil producing string, study on the basic types of oil producing wells and well completion was a necessity.

2.1 Types of Oil Producing Well

Development or producing well is a hole drilled through the Earth's surface designed to find or produce petroleum oil hydrocarbon from the reservoir. The life cycle of an oil production string may lasts up to more than 50 years and corrosion is one of the factors that shorten the life cycle of the facilities [5].

Study on the CO₂ corrosion in oil producing string is crucial since numerous amount of carbon dioxide (CO₂) gas is produced along with the oil. There are 3 types of oil producing well. The details of these wells are as shown below.

2.1.1 Vertical Well

The most common oil producing wells are drilled vertically (refer to Figure 1.1). This is generally the least expensive option to penetrate a single target. If the surface location is not fixed then the rig can be placed above the desired target to allow a vertical penetration to the desired reservoir location. A vertical well can also be drilled through several stacked reservoirs to produce through the vertical wellbore [3].

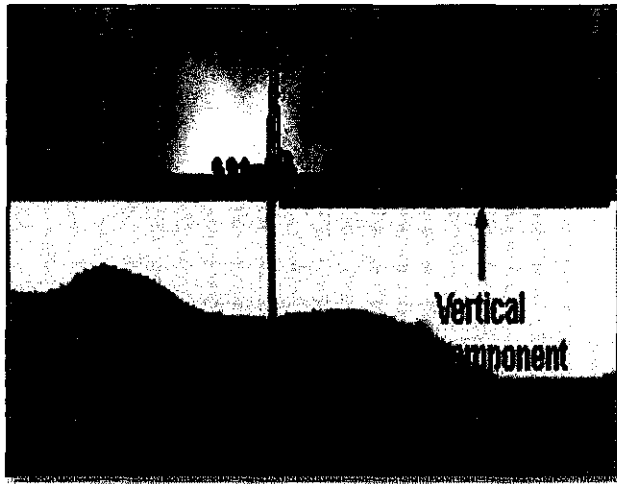


Figure 2.1: Directional/ Vertical Well

2.1.2 Deviated Well

A normal deviated well (single bore, less than 60° inclination) is the most common type of well currently drilled (refer to Figure 1.2). Many development wells are drilled as a group of wells from a single surface location and this requires directional wells for optimum spacing in the reservoir [3].

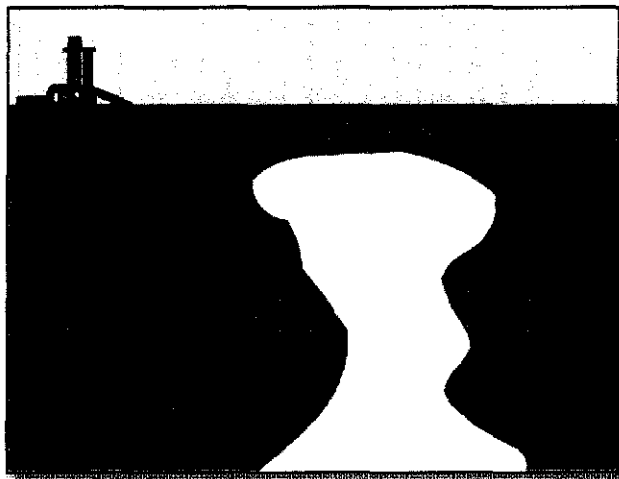


Figure 2.2: Deviated Well

2.1.3 Horizontal and Multilateral Well

Horizontal and multilateral wells (refer to Figure 1.3) have gained enormously in popularity. This type of well provide a lot of advantages compared to the

other types since it improves the surface of area contact between the wellbore and the formation [6]. Thus, it will enhance the production to the optimum.

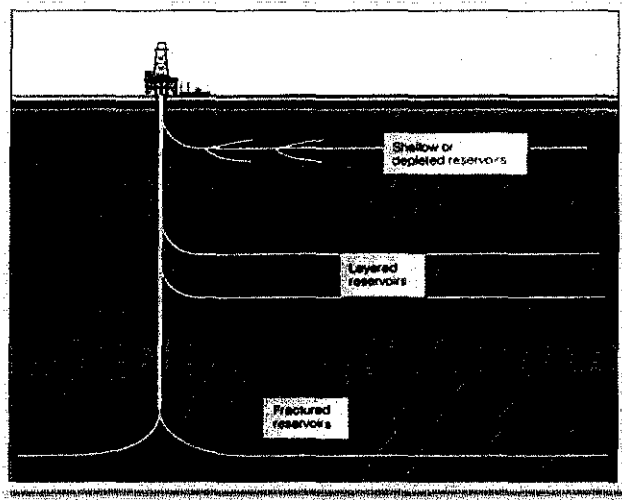


Figure 2.3: Horizontal and Multilateral Well

2.2 Components of a Typical Oil Producing Well

The typical type of oil producing well completion is the Cased, Cemented and Perforated Completion (refer to Figure 1.4) [3]. This type of completion is the most common because of its ability to effectively isolate the producing zone and by-pass the damaged portion of the bore hole. Either casing or liner is run across the reservoir and cemented into place, providing excellent hole protection.

Production tubing is run in the casing as close as possible to the reservoir and the reservoir section isolated using packers. The casing/liner across the reservoir section is then perforated (by-passing the filter cake and damaged zone), allowing production of the hydrocarbons [6]. Typical well completion consists of:

- a. Wellhead
- b. Casing
- c. Tubing
- d. Production Packer

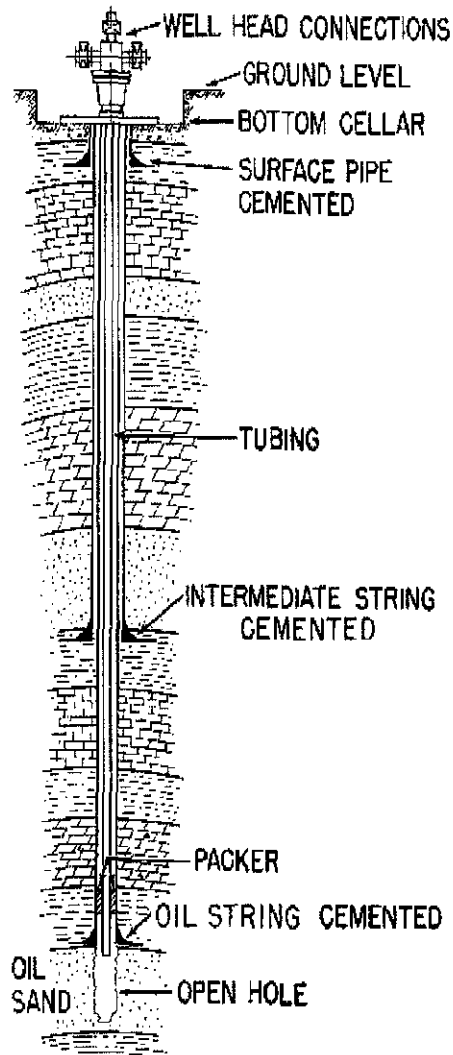


Figure 2.4: Cased, Cemented and Perforated Completion

2.2.1 Wellhead

Wellhead or Christmas Tree is the equipment installed at the surface of the wellbore to suspend the casings string. It consist of casing and tubing head, casing and tubing hangers, packoff and isolation seals, blow-out preventors and several valves. The functions of a wellhead are to suspend the string, casing pressure isolation and provide well access.

Wellhead components are mainly made of carbon steel and stainless steel [5]. Most of the external corrosion problem at wellhead is due to the existence of oxygen (O_2) at the surface. CO_2 corrosion mainly occurred on the internal surface of the wellhead.

2.2.2 Casing

Casing is a steel pipe which is run into the hole and cemented in place. Casing is used to protect a section of drilled hole and to provide a pressure vessel for drilling deeper and/or containing the production tubing strings through which hydrocarbons flow as the well is produced. Table 1.1 below shows different types of casing string.

Table 2.1: Casing Intervals

Types	Size (inch)
Conductor casing	30
Surface casing	28
Intermediate casing (optional)	13
Production casing	9

The conductor casing serves as a support during drilling operations, to flowback returns during drilling and cementing of the surface casing, and to prevent collapse of the loose soil near the surface. The surface casing is to isolate freshwater zones so that they are not contaminated during drilling and completion. The intermediate casing may be necessary on longer drilling intervals where necessary drilling mud weight to prevent blowouts may cause a hydrostatic pressure that can fracture deeper formations. The production casing string extends to the surface where it is hung off.

Few wells actually produce through casing, since producing fluids can corrode steel or form deposits such as asphaltenes or paraffins and the larger diameter can make flow unstable [6].

Most of the casing string is made of API J-55, K-55, N-80 or H-40 steel. The material may corrode over time and potentially expose to CO₂ corrosion since the string is on the sub surface. However, the casing string is sealed and isolated from any contact to the environment by cementing process. CO₂ corrosion may occur in the casing string if the cementing process is not done properly and caused communications between the casing and the seawater.

2.2.3 Production Packer

A production packer is a standard component of the completion hardware of oil or gas production wells used to provide a seal between the outside of the production tubing and the inside of the casing, liner, or wellbore wall [6]. Based on its primary use, packers can be divided into two main categories:

- a. Production packers
- b. Service packers.

Production packers are those that remain in the well during well production. Service packers are used temporarily during well service activities such as cement squeezing, acidizing, fracturing and well testing.

Material used in construction of production packer is stainless steel with 9% or higher chromium which is highly resistance to the CO₂ corrosion. Most of the corrosion problem encountered in the production packers is due to bimetallic or galvanic corrosion since the packers are in contact with different material used in casing or tubing string [1].

2.2.4 Tubing

Production tubing is a tubular used in a wellbore through which production fluids are produced. Production tubing provides a continuous bore from the production zone to the wellhead. It is usually between five and ten centimeters in diameter and is held inside the casing through the use of expandable packing devices. If there is more than one zone of production in the well, up to four lines of production tubing can be run [3].

Production tubing is used without cement in the smallest casing of a well completion to contain production fluids and convey them to the surface from an underground reservoir. The production tubing has a direct contact to the production fluids where CO₂ and water may be produced along with oil and CO₂ corrosion is a main threat to the tubing steel.

The production tubing material is made of API L-80 steel. The chemical composition of the steel is shown in Table 1.2 below. Figure 1.5 below shows the API L-80 steel that the student acquired from PETRONAS Carigali Sdn. Bhd. (PMO).

Table 2.2: Chemical composition of API L-80 steel

Element	Composition (%)
Carbon	0.15-0.21
Silicon	0.16-1.0
Manganese	0.35-1.0
Chromium	10.4-14.0
Phosphorus	max 0.020
Sulphur	max 0.0050
Aluminium	0.025-0.050
Ferum	remainder

The minimum yield strength = 80 000 psi

The maximum yield strength = 95 000 psi

The minimum tensile strength = 95 000 psi

The hardness = 23 HRC

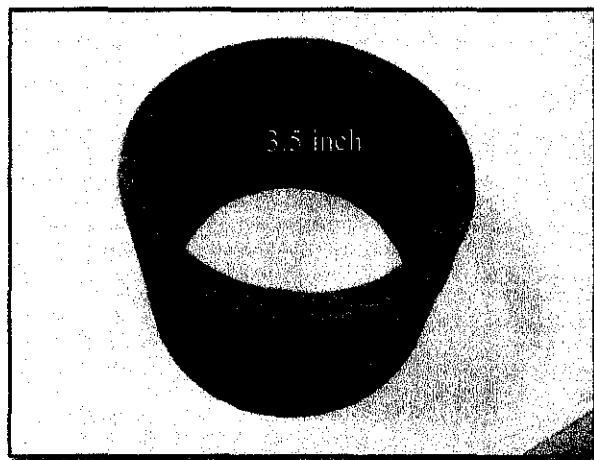


Figure 2.5: API L-80 steel

Most of the oil producing well in Malaysia is gas-lifted well or high gas oil ratio (GOR) well. In the gas-lifted well, the CO₂ corrosion is more likely to occur at the connection of gas lift valves and the tubing surface. The natural gas that used

to enhance the oil production contains numerous amount of carbon dioxide (CO_2) gas. As for the high GOR wells, carbon dioxide (CO_2) gas is highly soluble in the producing fluids where water and other gases is produced along the oil. The detail about the particles flow in the producing fluids is discussed in Section 2.3. When the CO_2 reacts with water, it becomes the ideal condition for CO_2 corrosion to occur. The details on the chemical reaction that leads to CO_2 corrosion is discussed in Section 2.4.

2.3 Particles Flow in the Oil Producing Well

Fluids and solid particles in the formations that flow up to the surface through the production tubing is the main contributor to the CO_2 corrosion problem in oil producing wells. Most of the wells produced raw liquid that is consists of oil, water, gas and some other solid particles such as sand.

2.3.1 Hydrocarbon

Hydrocarbon or petroleum oil originates from a small fraction of the organic matter deposited in sedimentary basins. Most of the organic matter is the remains of plants and animals that lived in the sea, and the rest is land-delivered organic matter carried in by rivers and continental runoff, or by winds [5]. These immediately condense into nitrogenous and humus complexes progenitors of kerogen. Some hydrocarbons are deposited in the sediments, but most form from thermal alteration at depth.

2.3.2 Gases

There are five (5) types of natural gas that is usually found in the production fluids [1]:

- a. Methane, CH_4
- b. Hydrogen Sulfide, H_2S
- c. Carbon Dioxide, CO_2
- d. Nitrogen, N_2
- e. Helium, He

Methane is formed by bacterial decay of organic material. It is a major product of the diagenesis of coal and is given off from all forms of organic matter during diagenesis [6]. Hydrogen sulfide originates from the reduction of sulfates in the sediments and from sulfur compounds in petroleum and kerogen. Carbon dioxide is derived from the decarboxylation of organic matter, and from HCO_3 and CaCO_3 . Nitrogen is derived from the nitrogen in organic matter and from trapped air. Helium is derived from the radioactive decay of uranium and thorium.

During the oil genesis and coalification process, the order of generation is generally carbon dioxide, nitrogen and methane. In most of the natural gases, the greatest individual component is methane typically 85 to 95% v/v. Levels of carbon dioxide (CO_2) are nominally 5% to 10% v/v. The combination of carbon dioxide (CO_2) gas and water is highly corrosive.

2.3.3 Produced Water

Produced water is water trapped in underground formations that is brought to the surface along with oil or gas. It is by far the largest volume by-product or waste stream associated with oil and gas production. On average, about 7 to 10 bbl produced water generated per 1 bbl of oil [5]. The formation structure indicates that most of the geological structure of the formation contains water which is the most efficient factor for the CO_2 corrosion in the oil producing wells.

There are 3 main elements in produced fluid; 1) Organic compounds such as grease, benzene, naphthalene and toluene. 2) Salts which primarily chlorides and sulfides. 3) Metal elements such as lead, chromium and nickel. In summary, produced waters are frequently one or all of the following:

- a. hot
- b. corrosive
- c. oily, waxy
- d. biologically active
- e. contain solids
- f. toxic

2.3.4 Solid Particle

Solids are also often present in produced fluids. They exist in many different forms, but principally originate from four individual sources:

- a. Drilling mud debris
- b. Reservoir sand
- c. Scales (both organic and inorganic)
- d. Corrosion products

Sand from the reservoir is the main contributor to the erosion corrosion in oil producing wells. CO_2 corrosion product, carbonate is one of the solid particles found in the produced fluids.

There are various types of corrosion that may occur in the oil producing well. Figure 1.6 below shows the components in typical oil producing well that are potential for corrosion to occur.

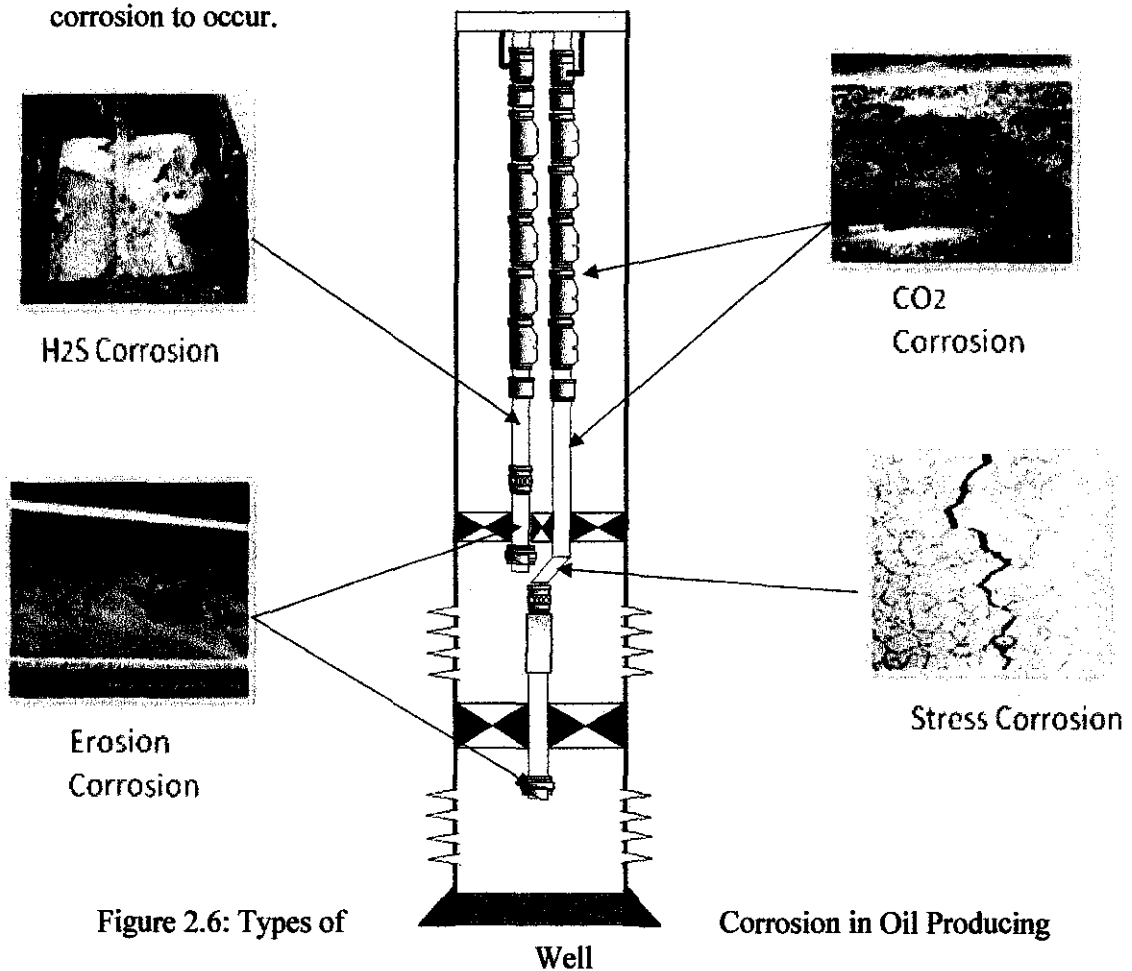


Figure 2.6: Types of

Corrosion in Oil Producing

2.4 Basic of CO₂ Corrosion

Dry CO₂ gas by itself is not corrosive at the temperatures encountered within oil and gas production systems [8]. It becomes corrosive when dissolved in an aqueous phase through which it can promote an electrochemical reaction between steel and the contacting aqueous phase. Various mechanisms have been postulated for the CO₂ corrosion process but all involve either carbonic acid (H₂CO₃) or the bicarbonate ion (2HCO₃⁻) formed on dissolution of CO₂ in water [10]. The step for the CO₂ corrosion process is presented by the reaction shown in the equations as follows:



The mechanism suggested by de Waard is:



With the steel reacting:



The overall equation is:



On the other hand, CO₂ corrosion results from the practice of pumping CO₂ saturated water into wells to enhance oil recovery and reduce the viscosity of the pumped fluid. The presence of CO₂ in solution leads to the formation of a weak carbonic acid which drives CO₂ corrosion reactions [10]. The initiating process is presented by the reaction shown in equation (2.6).



The following corrosion process is controlled by three cathodic reactions and one anodic reaction. The cathodic reactions, include (2.7a) the reduction of carbonic acid into bicarbonate ions, (2.7b) the reduction of bicarbonate ions, and (2.7c) the reduction of hydrogen ions.



The anodic reaction significant in CO₂ corrosion is the oxidation of iron to ferrous (Fe²⁺) ion given in equation (2.8).



These corrosion reactions promote the formation of FeCO₃ which can form along a couple of reaction paths. First, it may form when ferrous ions react directly with carbonate ions as shown in equation (2.9). However, it can also form by the two processes shown in equations (2.10a, 2.10b). When ferrous ions react with bicarbonate ions, ferrous iron bicarbonate forms which subsequently dissociates into iron carbonate along with carbon dioxide and water.



CO₂ = Carbon Dioxide

H₂ O = Water

H₂ CO₃ = Carbonic Acid

Fe = Iron

FeCO₃ = Iron Carbonate (corrosion product)

H₂ = Hydrogen

The significance of FeCO₃ formation is that it drops out of solution as a precipitate due to its limited solubility. This precipitate has the potential to form passive films on the surfaces of steel which may reduce the corrosion. [9]

2.4.1 Types of CO₂ Corrosion Failure

In oil producing wells, CO₂ corrosion have always presented as a severe problem to the production tubing. Most of the cases, corroded tubing may deplete the production and need very high cost maintenance to rectify the problem [1]. In addition, the risk of pollution and hazards to safety are the important reasons for adequate further on corrosion study. Below are the lists of effect due to carbon dioxide corrosion to internal tubing surface:

a. Pitting

Pitting is defined as corrosion of a metal surface, confined to a point or small area that takes the form of cavities [9]. Pitting can occur over the full range of operating temperatures under stagnant to moderate flow conditions. Pitting may arise close to the dew point and can relate to condensing conditions. The susceptibility to pitting increases and time for pitting occur decrease with increasing temperature and increasing CO₂ partial pressure.

b. Mesa type attack

It is a form of localized CO₂ corrosion occurs under medium flow conditions where the formation of protective FeCO₃ film layers is unstable. Film formation begins around 60°C and thus mesa attack is much less of a concern at temperatures below this [9]. The type of this attack most encountered in the area which is has high fluid turbulence such as welds, tubing joints, or ends/constrictions in piping.

c. Flow induced localized corrosion (FILC)

The damage is an extension of pitting and mesa attack above critical flow intensities. The localized attack propagates by local turbulence created by pits and steps at the mesa attack which act as flow disturbances. The local turbulence combined with these stresses inherent in the scale may destroy existing scales. The flow conditions may then prevent protective FeCO₃ film layers on the exposed metal to reform again.

2.4.2 CO₂ Corrosion Prevention Method

To know the fact that CO₂ corrosion phenomenon cannot be eliminated in oil producing wells, the only way to reduce the problem is to minimize as much as possible the effect and severity caused by CO₂ corrosion. The lists below are some of the CO₂ corrosion prevention method that are widely use in oil and gas industry.

a. Corrosion Inhibitor

A corrosion inhibitor is a chemical compound that, when added to a fluid or gas, decreases the corrosion rate of a metal or an alloy [15]. The corrosion inhibition efficiency of a corrosion inhibitor is a function of many factors such as fluid composition, quantity of water and flow regime. In oil producing wells, the oil itself may be the inhibitor if the produced fluids GOR is low. But in most of the cases, corrosion inhibitor such as hydrazine and ascorbic acids is injected into the production tubing periodically to decrease the corrosion rate.

b. Cathodic Protection

Cathodic protection (CP) is a technique to control the corrosion of a metal surface by making it work as a cathode of an electrochemical cell. This is achieved by placing in contact with the metal to be protected another more easily corroded metal to act as the anode of the electrochemical cell. Cathodic protection interferes with the natural action of the electrochemical cells that are responsible for corrosion [15]. Cathodic protection can be effectively applied to control corrosion of surfaces that are immersed in water.

c. Protective Coating

Protective coatings are the most widely used corrosion control technique. Essentially, protective coatings are a means for separating the surfaces that are susceptible to corrosion from the factors in the environment which cause corrosion to occur. However, the protective coatings can never provide 100 percent protection of 100 percent of the surface [15]. Coatings are particularly useful when used in combination with other methods of corrosion control such as cathodic protection.

2.5 Tests for CO₂ Corrosion

In order to study and analyze the CO₂ corrosion rate in API L-80 steel, two (2) methods of laboratory test are conducted.

2.5.1 Weight Loss Method using Autoclave

Weight loss measurement is the most widely used means of determining corrosion loss, despite being the oldest method currently in use [12]. A Weight sample (coupon) of the metal or alloy under consideration is introduced into the process, and later removed after a reasonable time interval. The coupon is then cleaned of all corrosion products and is reweighed. The weight loss is converted to a corrosion rate or metal loss. The technique requires no complex equipment or procedures, merely an appropriately shaped coupon, a carrier for the coupon (coupon holder), and a reliable means of removing corrosion product without disruption of the metal substrate.

The method is commonly used as a calibration standard for other means of corrosion monitoring, such as Linear Polarization Resistance Method. In instances where slow response and averaged data are acceptable, weight loss monitoring is the preferred technique. The Weight loss method tests are to be conducted using Autoclave Corrosion Test Equipment (refer to Figure 2.7) to determine the CO₂ corrosion rate in API L-80 steel.

Autoclave corrosion tests are a convenient means for laboratory simulation of many service environments for the purpose of evaluating corrosion resistance of materials and for determining the effects of metallurgical, processing, and environmental variables on corrosion processes. The reason for such tests is to more closely recreate the high temperature and pressure commonly occurring in commercial or industrial processes. In most situations involving aqueous corrosion, it involves a water-based solution containing various dissolved salts such as chlorides, carbonates, bicarbonates, alkali salts, acids and other constituents [7].

Using Autoclave, high temperature and high pressure corrosion test in static condition is possible to be conducted under the environment as mentioned above which is simulating the actual condition in oil producing well.

The Autoclave Corrosion Test Equipment is designed to specification given in the ASME Boiler and Pressure Vessel Code and meets the ASTM G 31, Practice for Laboratory Immersion Corrosion Testing of Metals standard.



Figure 2.7: Autoclave Corrosion Test Equipment

2.5.2 Linear Polarization Resistance Method

Linear Polarization Resistance Monitoring (LPR) technique is the most efficient way to measure corrosion rate [14]. It is the only corrosion monitoring method that allows corrosion rates to be measured directly in real time. This method is useful to rapidly identify corrosion upsets and initiates remedial action in water-based, corrosive environments.

In the typical LPR technique, a potential (typically of the order of 10-20 mV) is applied to a freely corroding sensor element and the resulting linear current response is measured [16]. This small potential perturbation is usually applied step-wise, starting below the free corrosion potential and terminating above the free corrosion

potential. The polarization resistance is the ratio of the applied potential and the resulting current response. This resistance is inversely related to the uniform corrosion rate.

The corrosion current I_{corr} , generated by the flow of electrons from anodic to cathodic sites, could be used to compute the corrosion rate by the application of a modified version of Faraday's Law:

$$C = \frac{I_{CORR} \times E}{A \times D} \times 128.67 \quad (3.1)$$

where:

C = Corrosion rate in "mils per year" (MPY)

E = Equivalent weight of the corroding metal (g)

A = Area of corroding electrode (cm²)

d = Density of corroding metal (g/cm³)

Anodic and cathodic sites continually shift position, and they exist within a continuously conductive surface, making direct measurement of I_{corr} impossible [16]. Small, externally-imposed, potential shifts (ΔE) will produce measurable current flow (ΔI) at the corroding electrode. The behavior of the externally imposed current is governed, as is that of I_{corr} , by the degree of difficulty with which the anodic and cathodic corrosion processes take place.

From the linear polarization resistance test, we can determine the corrosion rate of the sample. The theory behind corrosion rate calculation is as mention below. The corrosion current density is related to polarization resistance by Stern_Geary coefficient, B. The Stern-Geary Constant, B, is approximated as 25 mV for all pH.

$$i_{corr} = B/R_p \quad (3.2)$$

The dimension of R_p is ohm-cm², i_{corr} is mA/cm², and B is in V. B also can be written as:

$$B = \frac{b_a b_c}{2.303(b_a + b_c)} \quad (3.3)$$

Where b_a , b_c is the Tafel slope for cathodic and anodic reaction. According to the software that we are using in the lab to do the calculation, Tafel Slope, B used in the calculation is 26.

The corrosion rate, CR in mm/year can be determined from the formula shown below:

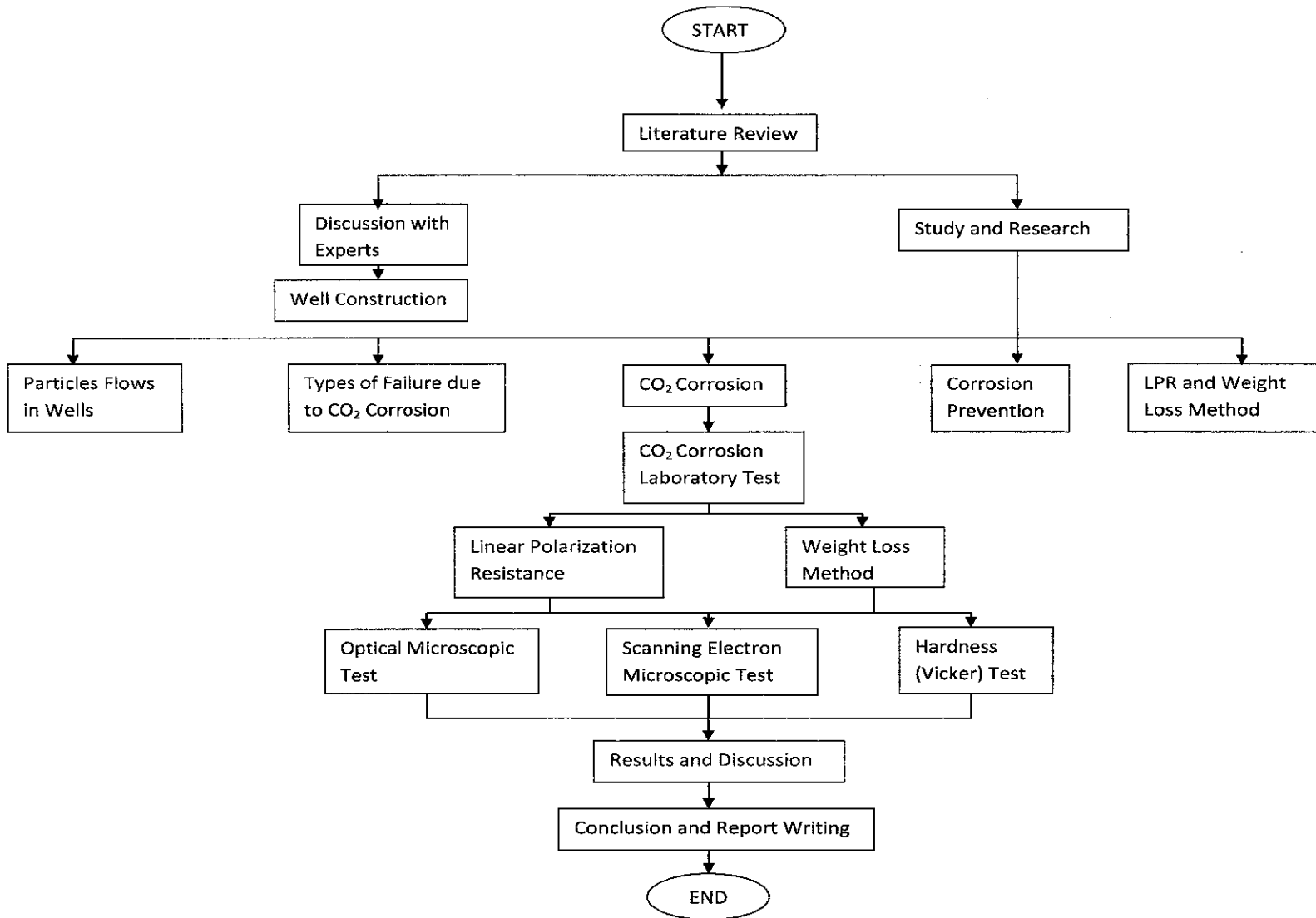
$$CR = 3.27 \times i_{\text{corr}} \text{EW} / \text{density of the corroding material} \quad (3.4)$$

where,

EW = equivalent weight of the corroding species in grams

**CHAPTER 3
METHODOLOGY**

3.1 Overall Project Flowchart



3.2 Weight Loss Method using Autoclave

A weighed sample, L-80 steel specimen was introduced into the process, and later removed after a reasonable time interval. The specimen was then cleaned of all corrosion products and reweighed. The weight loss was converted to a corrosion rate (CR) or metal loss (ML), as follows:

$$\text{Corrosion Rate (CR)} = \frac{\text{Weight loss (g)} \cdot K}{\text{Alloy Density (g/cm}^3) \cdot \text{Exposed Area (A)} \cdot \text{Exposure Time (hr)}}$$

Table 3.1: The constant values to calculate the corrosion rate in various units

Desired Corrosion Rate Unit (CR)	Area Unit (A)	K-Factor
mils/year (mpy)	in ²	5.34 x 10 ⁻⁵
mils/year (mpy)	cm ²	3.45 x 10 ⁻⁶
millimeters/year (mmy)	cm ²	8.76 x 10 ⁻⁴

$$\text{Metal Loss (ML)} = \frac{\text{Weight loss (g)} \cdot K}{\text{Alloy Density (g/cm}^3) \cdot \text{Exposed Area (A)}}$$

Desired Metal Loss Unit (ML)	Area Unit (A)	K-Factor
mils	in ²	61.02
mils	cm ²	393.7
millimeters	cm ²	10.0

Cleaning of specimens before weighing and exposure was critical to remove any contaminants that could affect test results [13]. Reference was made to NACE Recommended Practice RP-0775 and ASTM G-1 & G-4 for further detail on surface finishing and cleaning of weight-loss coupons. The experiments are to be conducted in Block I using Autoclave Corrosion Test Equipment using ASTM G-31, Practice for Laboratory Immersion Corrosion Testing of Metals as the reference.

3.2.1 Preparation of Specimen/Coupon

The material used for the experiment (L80 steel) was supplied by PETRONAS Carigali Sdn. Bhd. (PMO). The chemical composition of alloys as obtained from the company data sheet are as shown in Table 3.1. The steel was cut and machined using wire cut method in lab into the rectangular specimens of dimension 15 x 10 x 5mm and 3mm diameter of hole was cut at the center (refer to Figure 3.1) to facilitate suspension of the sample inside the Autoclave.

All faces of the samples were initially coarsed ground on SiC belt grinder machine then consequently machine polished to 800-grade finish using silicon carbide paper. The polished samples were washed and subsequently washed in acetone. 15 sets of specimens were prepared for the test.

Table 3.2: Chemical Composition of API L-80 Specimen

GRADE	C	Mn	Si	S	P	Cr	Mo
L-80	0.22	1.38	0.22	0.21	0.28	0.013	0

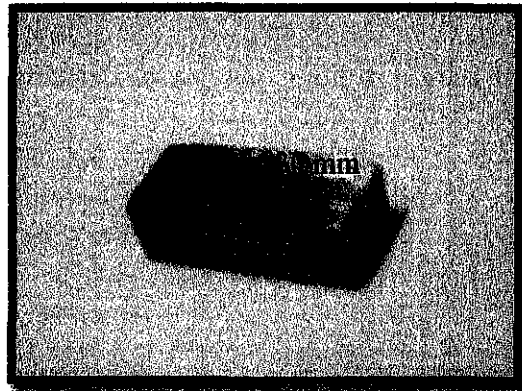


Figure 3.1: L-80 Steel Specimen for Weight Loss Method using Autoclave

3.2.2 Preparation of Solutions

The solutions were prepared from the 1 litre of deaerated water mixed with NaCl to achieve the 3% NaCl solution. The pH of the solution was adjusted to the pH=5. The pH value was checked by microcomputer pH-meter METTLER-TOLEDO Model 320, which had been calibrated using standard buffer.

3.2.3 Laboratory Setup

The set-up for the Weight loss laboratory test using Autoclave was showed in Figure 3.2 and Figure 3.3. The test assembly consists of Autoclave equipment, CO₂ gas supplier and a computer for data acquisition.

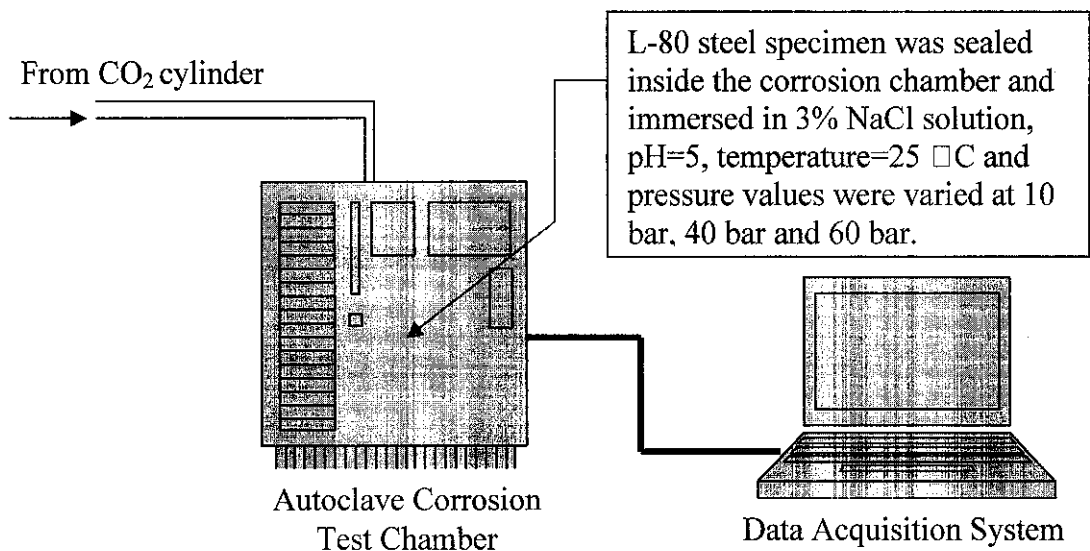


Figure 3.2: Schematic Diagram for Weight Loss Method using Autoclave

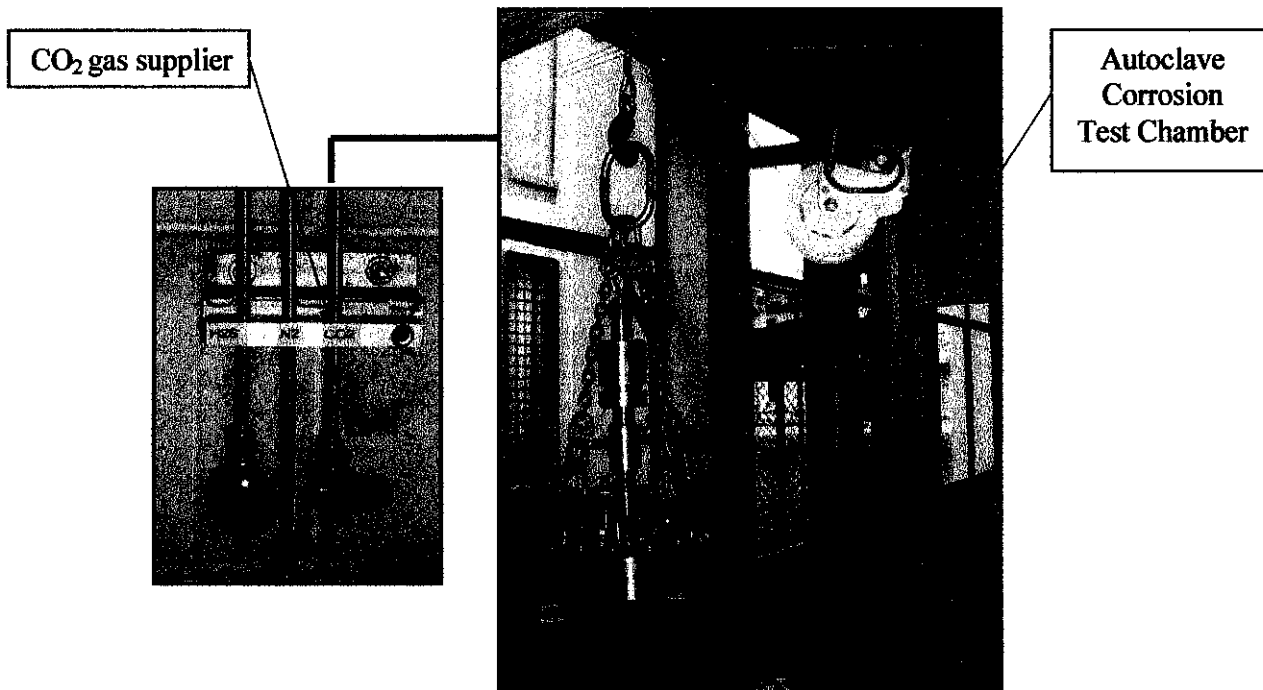


Figure 3.3: Real Weight Loss Method using Autoclave Test Setup

3.2.4 Experiment Procedures for Weight Loss Method using Autoclave

The temperature of solution used was constant at room temperature, 25 °C. The pressure during the experiment was varied from 10 to 60 bar which is in the range of actual pressure condition in oil producing well (Tukau 45L) as provided by Production Technologist of PETRONAS Carigali Sdn. Bhd. The pressure value was controlled from the computer. The values of pressure of the solution used were:

- a. 10 bar
- b. 40 bar
- c. 60 bar

Experiments procedures were as per described below:

- a. Test solution and the test specimen were prepared as mentioned above. 1 liter of test solution where the temperature was maintained at 25 °C within 1 °C was prepared 1 hour before run the experiment.

The specimen prepared as per describe in Section 3.2.1 and setting up of the equipment for the laboratory test as per describe in Section 3.2.3.

- b. Initial weights of the samples were measured using microbalance equipment. The average value of each sample was noted.
- c. The Autoclave corrosion chamber was deaerated by using a pump vacuum and purging argon continuously for 1 hour to remove the oxygen impurity.
- d. Then, the test solution was poured into the AutoClave corrosion chamber.
- e. Three sets of coupons were placed hanging in the chamber to avoid any contact with any material that may caused galvanic caorrosion.
- f. The chamber was then sealed using bolts and nuts.
- g. The pressure was raised to 10 bar by charging CO₂ gas into the chamber. The process was controlled by the digital display unit (DDU) in the computer. SmartCET software from Honeywell was used to control and for data acquisition during the experiment.
- h. The experiment was kept running for 48 hours continuously.
- i. Experiment for 40 bar and 60 bar pressure were conducted using the same procedure as mention above.
- j. In order to analyze the corrosion products, scanning electron microscopic (SEM) was used on the coupons after each of the experiment.
- k. Micro hardness test was conducted later to measure the effect of CO₂ corrosion to the coupons.

3.3 Linear Polarization Resistance Method

Linear Polarization Resistance Method was used to determine the corrosion rate of metal in a specific environment. ASTM 59, Standard Method in Conducting Potentiodynamic Polarization Resistance Measurements described the experimental procedure for polarization resistance method which can be used for calibration of equipment and verification of experimental technique.

The test method can be utilized to verify the performance of polarization resistance measurements equipments. Polarization resistance can be related to the rate of general corrosion for metal at or near the corrosion potential, it is an accurate and rapid way to measure the general corrosion rate. The test procedures standard included were:

- a. Test solutions were prepared, and the standard test cell requires 900ml of test solution where the temperature was maintained at 30 °C within 1 °C.
- b. Test cell was purged at 150 cm³/min before specimen immersion and continue throughout the test.
- c. Working electrode was prepared, and experiment was conducted within 1 hour of the preparing electrode. Preparation including sequential wet polishing with 240 grit and 600 grit SiC paper. Surface area of the specimen was determined to the nearest of 0.01 cm² and subtract the area under the gasket.
- d. Prior to immersion of the specimen, it was degreased with acetone and rinsed with distilled water. The time delay between rinsing and immersion was kept minimal.
- e. The test specimen was transferred into test cell and position the probe tip to 2 to 3 mm from the test electrode surface. The diameter of the tip was not more than 1 mm.

3.3.1 Preparation of the Working Electrode

The samples (L80) were cut into 2cm diameter cylinder and spot welded with copper wire. Then, it was mounted with epoxy by cold mounting and then polished to 800-grade finish using silicon carbide paper. Finally, it was degreased and rinsed with deionizer water and ethanol. The working electrode is as shown below.

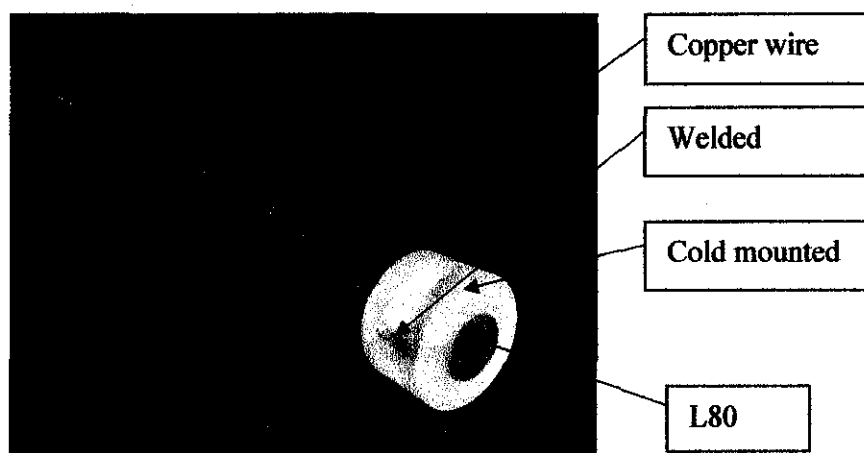


Figure 3.4: Working Electrode used in the LPR Test

3.3.2 Preparation of Solutions

The solutions were prepared from the 3% NaCl solution was saturated with CO₂ by purging for one hour prior to the exposure of electrode. The pH of the solution was adjusted by adding an amount of sodium hydrogen carbonate. The pH value was checked by microcomputer pH-meter METTLER-TOLEDO Model 320, which had been calibrated using standard buffer.

3.3.3 Laboratory Setup

The set-up for the laboratory test using electrochemical measurement using linear polarization resistance method is showed below. The test assembly consist of one liter glass cell bubbled with CO₂ gas. The required test temperature was set through hot plate. The electrochemical measurements were based on a three-electrode system. The reference electrode used was a saturated calomel electrode (SCE) and the auxiliary electrode was a platinum electrode. Figure 3.5 shows the schematic diagram of the test and Figure 3.6 shows the real test setup in laboratory.

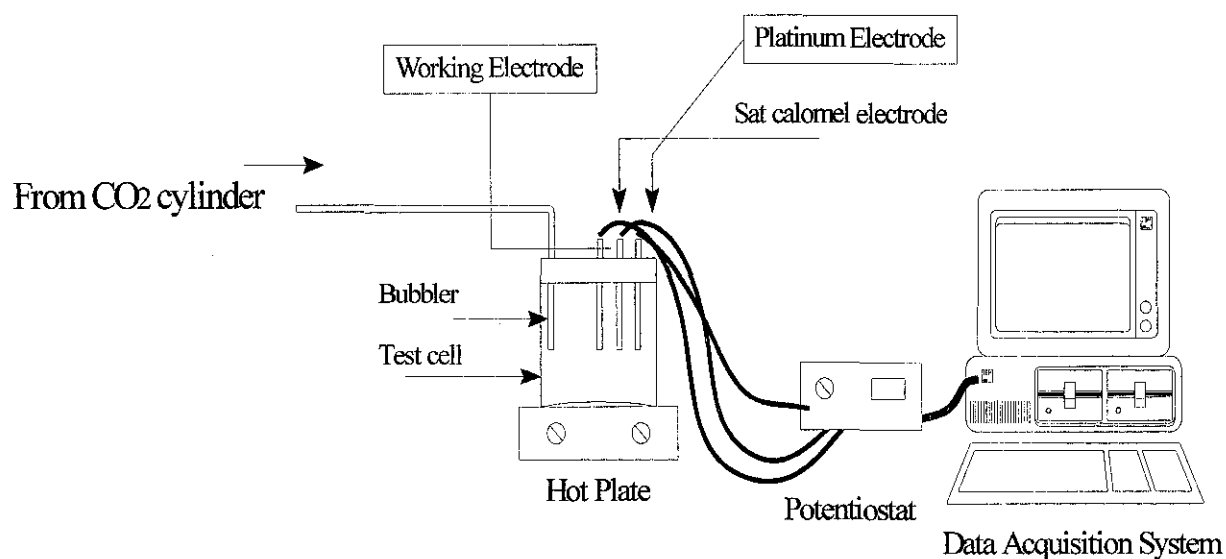


Figure 3.5: Schematic Diagram of LPR Test



Figure 3.6: Real LPR Test Setup in Laboratory

3.3.4 Experiment Procedures for Temperature and Rotational Rate Parameters using LPR

The temperature of solution used was varied from 60 to 120 °C. The rotational rate during the experiment was varied from 0 to 6000 rpm. The pressure was constant at atmospheric pressure, 1 atm. The temperature values and the rotational rate values were within the range of actual condition in oil producing well (Tukau 45L) as provided by Production Technologist of PETRONAS Carigali Sdn. Bhd. Hot plate was used to control the temperature at constant value throughout the experiment. The values of temperature of the solution used were:

- a. 25 °C
- b. 40 °C
- c. 60 °C

The values of rotational rate used were:

- a. 0 rpm
- b. 1000 rpm
- c. 2000 rpm
- d. 4000 rpm
- e. 6000 rpm

Experiments procedures were as per described below:

- a. Solution medium of sodium chloride 3% prepared, 30g of sodium chloride was mixed into the distilled water of 1 liter.
- b. Working electrode prepared as per describe in the Section 3.3.1 and setting up of the equipment for the laboratory test as per described in Section 3.3.3.
- c. Purging of the carbon dioxide gas started and continuous purging for half an hour until the carbon dioxide was saturated in the solution. The indication of the cell was saturated with carbon dioxide was tested with the pH meter when it indicated the reading of pH nearly 3.8.
- d. The solution was then heated up to 25°C to provide the desired temperature for the experiment, and sodium bicarbonate was added into the solution to increase the pH of the solution to 5. The pH value was constant throughout the experiment for temperature parameter. Once, the environment of the experiment achieved.
- e. For the first section of the experiment, the solution was maintained at 25°C at rotational rate 0 rpm. After one hour of test run, the result yielded from the experiment was noted and run for another hour. This procedure was repeated for the rotational rate value at 1000 rpm, 4000 rpm and 6000 rpm. Proceed to step (h).
- f. Second section of the experiment was using 40°C as the solution temperature and rotational rate at 0 rpm. The hot plate was set at 40°C and then maintained on the test run for 1 hour. The results and output graph yield for the next 1 hour was noted. This procedure was repeated for the rotational rate value at 1000 rpm, 4000 rpm and 6000 rpm. Proceed to step (h).
- g. Third section of the experiment was using 60°C as the solution temperature and rotational rate at 0 rpm. The hot plate was set at 60°C and then maintained on the test run for 1 hour. The results and output graph yield for the next 1 hour was noted. This procedure was repeated for the rotational rate value at 1000 rpm, 4000 rpm and 6000 rpm. Proceed to step (h).
- h. Once the working electrode was added into the solution, the data acquisition system yielded the results. Then, Gill 12 Weld Tester Serial No. 1350 – Sequencer and the Core Running software was run.

- i. Then, ACM Instruments was run and data was gathered automatically into the ACM Analysis, where it recorded down the Linear Polarization Resistances and calculated the corrosion rate using the formula.

3.4 Scanning Electron Microscopic (SEM)

The SEM test was conducted to analyze the corrosion products at the specimens after each experiment. The SEM machine is attached with EDM equipment where the chemical composition of the L-80 steel can be detected. All of the specimens were sealed and sent to the SEM lab within 1 hour prior to the test. The test was conducted by lab technician in UTP Academic Block, Building 17 because of the high cost and high radiation emitted during the test.

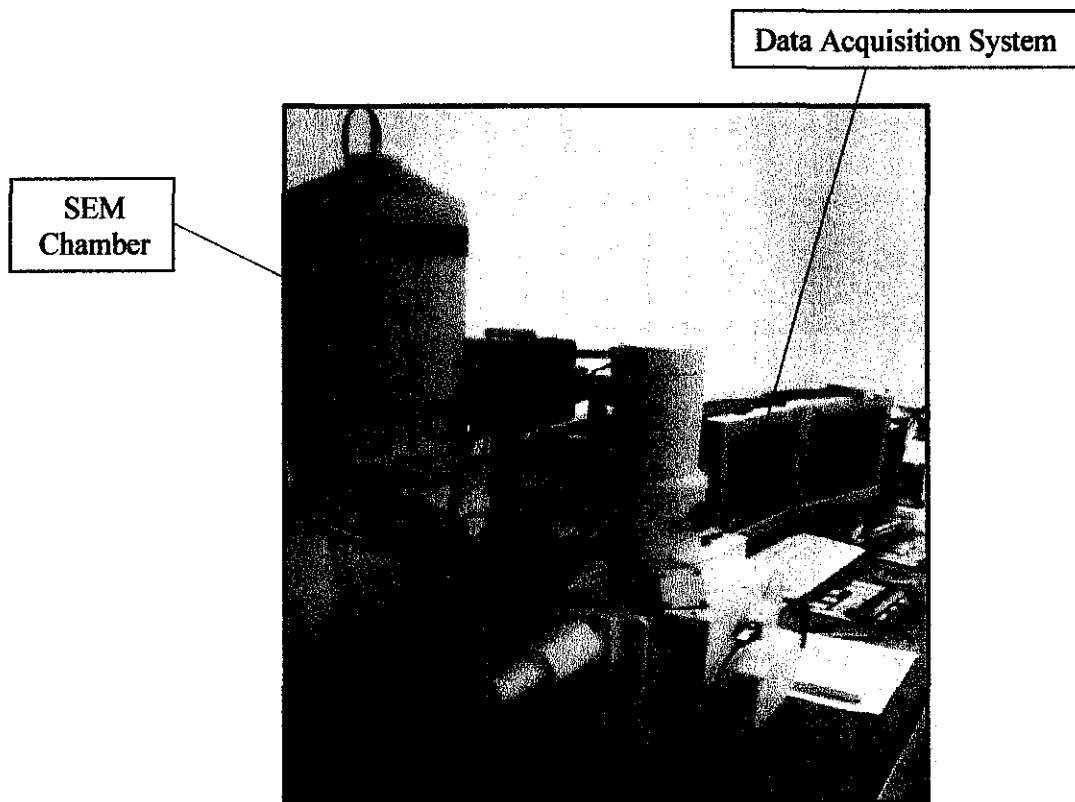


Figure 3.7: SEM Machine

3.5 Optical Microscopic Test

Optical Microscopic Test was conducted to analyze the surface condition of the specimens after each experiment. The tests procedures were as shown below:

- a. After completed the Weight Loss Method, Linear Polarization Method and SEM test, the specimens were sealed in vacuum.
- b. The specimens were cleaned with ethanol.
- c. Then, nital (etchant) was used to the specimens prior to 1 minute before conducting optical microscopic test.
- d. The surface condition of each specimen was recorded by a computer for data acquisition.

3.6 Microhardness (Vicker) Test

The test was conducted to analyze the effect of CO₂ corrosion to the hardness of the material. The specimen's microhardness was tested before and after corrosion. The parameters used during the test are as shown below:

- a. Test Load = 50 gf
- b. Dwell Time = 15 seconds

The test procedures were as mentioned below:

- a. The test specimens were mounted using the Auto Mounting Press Machine to achieve a flat surface as a requirement to conduct the Microhardness Test.
- b. Then, the flat face of the specimens were coarse ground on SiC belt grinder machine until 1200 grit silicon carbide paper and consequently polished using 6 grade and 1 grade diamond paste.
- c. The specimens were washed using ethanol and prepared for the test.
- d. The specimen was placed under a microscope and positioned until it shows the grain structure of the material. 50 gf load test was applied to the specimen until a 'diamond shaped' on the surface can be seen from the microscope.
- e. The length of the diamond hole was measured and the Microhardness Test Machine automatically calculated the material's hardness in HV units.

CHAPTER 4

RESULTS AND DISCUSSION

4.1 Actual Data from Tukai 45L Oil Producing Well

To conduct the tests based on actual condition in oil producing well, the author managed to receive some data from PETRONAS Carigali Sdn. Bhd (SKO). Tests conducted were to simulate the actual condition of Tukai 45L oil producing well in Tukai Field, Sarawak. The oil is producing from the 2-F6/G2 reservoir. Table 4.1 shown below is the results from the Flowing Gradient Survey that was conducted at the oil producing well on 6th October 2008 using wireline operation. Figure 4.1 and Figure 4.2 below show that the value of temperature and pressure during the production. The data provided was used as a reference to the value of parameters used during the experiment.

Table 4.1: Data Acquired from FGS Operation in Tukai 45L Well

FLOWING GRADIENT SURVEY								
FIELD	: TUKAU	START OF SURVEY	: 6/10/2008					
WELL	: TK 45L	DERRICK FLOOR ELEVATION	: 92.0 FT. AMSL					
RESERVOIR	: 2-F6/G2	TOP BOTTOM FLANGE	: 50.0 FT. BDF					
		PERFORATIONS	: 3088' - 3199' FT. BDF					
CORRECTED								
	AH DEPTH (FT BDF)	TV DEPTH (FT SS)	TV DEPTH (FT SS)	TEMP (DEG F)	PRESSURE (PSIA)		GRADIENT (PSI/FT. SS)	
	L.E *	L.E	L.E		U.E	L.E.	U.E.	L.E.
1st lubr.	50.0	-42.0		96.7	124.3	124.7		
flw. grad	465.0	372.8		118.1	163.5	164.6	0.094	0.096
flw. grad	665.0	572.6		119.7	180.9	180.8	0.087	0.081
flw. grad	865.0	772.5		121.2	192.5	193.6	0.058	0.064
flw. grad	885.0	792.5		121.5	205.8	205.3	0.665	0.585
flw. grad	1195.0	1101.9		123.5	233.9	234.8	0.091	0.095
flw. grad	1505.0	1407.9		125.3	268.7	268.8	0.114	0.111
flw. grad	1525.0	1427.4		125.4	270.7	270.2	0.103	0.072
flw. grad	1740.0	1634.8		126.3	295.4	295.1	0.119	0.120
flw. grad	1960.0	1844.3		127.2	323.8	324.2	0.136	0.139
flw. grad	1980.0	1863.3		127.6	327.4	327.0	0.189	0.147
flw. grad	2490.0	2353.5		132.9	513.1	512.2	0.379	0.378
flw. grad	2960.0	2794.3		136.7	686.8	686.0	0.394	0.394
flw. grad	3065.0	2889.6		136.9	725.9	725.9	0.410	0.419
flw. grad	3100.0	2921.3		136.9	737.9	737.4	0.378	0.363
2nd lubr.	50.0	-42.0		104.1	132.7	133.9	0.204	0.204

* DEPTH U.E. = (DEPTH L.E. - 2.0) FT

Laboratory tests were conducted using the data above. The test matrixes for each test are as shown below. All tests were using API L-80 steel specimen.

- a. Laboratory experiment to determine the CO₂ corrosion rate in L80 steel under static condition using Autoclave Weight Loss Method with varied pressure (10 bar, 40 bar and 60 bar), in 3% NaCl solutions, at room temperature (25°C) and pH5. Pressure value from Tukai 45L oil producing well; 100 to 750 psi which is approximately equals to 7 to 51 bar.
- b. Laboratory experiment to determine the CO₂ corrosion rate in L80 steel using Linear Polarization Method with varied temperature (25°C, 40°C and 60°C) and varied rotational rate (0 rpm, 1000 rpm, 2000 rpm, 4000 rpm and 6000 rpm), in 3% NaCl solutions, at atmospheric pressure (1 atm) and pH5. Temperature value from Tukai 45L oil producing well; 95 to 140 Fahrenheit which is approximately equals to 35 to 60 °C.
- c. Laboratory experiment to analyze the corrosion product and surface condition before and after corrosion occurs, SEM and OM test.
- d. Laboratory experiment to analyze the effect of CO₂ corrosion on the material's hardness.

4.2 Weight Loss Method using Autoclave Test Results

Three sets of experiments with two specimens each were conducted. The first experiment was conducted at 10 bar pressure environment. The second experiment was conducted at 40 bar pressure and the third experiment at 60 bar pressure environment. Table 4.2 below shows the average weight different (gram) of the specimens with the respective pressure.

Table 4.2: Average Weight Differences in API L-80 Steel Specimens

	10 bar	40 bar	60 bar
Specimen 1 (gram)	0.0055	0.0093	0.0096
Specimen 2 (gram)	0.006	0.0082	0.011

Based on the theory explained in the previous section, the corrosion rate is calculated by the formula:

$$\text{Corrosion Rate (CR)} = \frac{\text{Weight loss (g)} \cdot K}{\text{Alloy Density (g/cm}^3) \cdot \text{Exposed Area (A)} \cdot \text{Exposure Time (hr)}}$$

where:

L80 steel density = 7.86 g/cm³

Exposed area = 5.5 cm²

Exposure time = 48 hours

K = 8.76 x 10⁴

The average CO₂ corrosion rate in tubing steel (API L-80) at 10 bar, 40 bar and 60 bar, in 3% NaCl solutions, at room temperature (25 °C) and solution pH5 using Autoclave Weight Loss method is shown as per Table 4.3 below:

Table 4.3: Average CO₂ Corrosion Rates in API L-80 Steel
from Weight Loss Method Test

Pressure	Corrosion rates (mm/yr)	
	Specimen 1	Specimen 2
10 bar	0.2334	0.254
40 bar	0.3905	0.347
60 bar	0.4044	0.4681

4.2.1 Weight Loss Method Test: Discussion

The experiment was conducted in static condition, immersed for 48 hours in CO₂ saturated 3% NaCl solution at pressure 10 bar, 40 bar and 60 bar and temperature is constant throughout the experiment at 25°C. The L 80 steel corrosion rate yields from the experiment is in the range of 2.3 x 10³ to 4.7 x 10³ mm/yr.

The trend is increasing with the increase of pressure values. It is known that in high pressure environment, the corrosion rate will increase due to local depletion of HCO₃⁻ ions which is favoring the cathodic reaction that can lead to corrosion.

The analysis on the specimen surface condition after the tests is discussed in Section 4.4 and Section 4.5 under the SEM and OM tests results.

4.3 Linear Polarization Resistance Method Tests Results

Based on the theory explained in the previous section, the corrosion rate is calculated by the data acquisition system using software called Gill 12 Weld Tester Serial No 1350- Sequencer. The corrosion rate result of the L80 steel at varied temperature (25 °C, 40 °C and 60 °C) and varied rotational rate (0 rpm, 1000 rpm, 2000 rpm, 4000 rpm and 6000 rpm), in 3% NaCl solutions, at atmospheric pressure (1 atm) and solution pH5 is shown in Table 4.4 and Figure 4.3.

Table 4.4: Average CO₂ Corrosion Rates in API L-80 Steel from LPR Test

Temperature (°C)/ Rotational Rates (rpm)	Average CO ₂ Corrosion Rates (mm/yr)		
	at 25°C	at 40°C	at 60°C
0	1.35	2.26	2.9
1000	1.44	2.31	3.14
2000	1.7	2.35	3.68
4000	2.03	2.41	3.85
6000	2.14	2.59	3.9

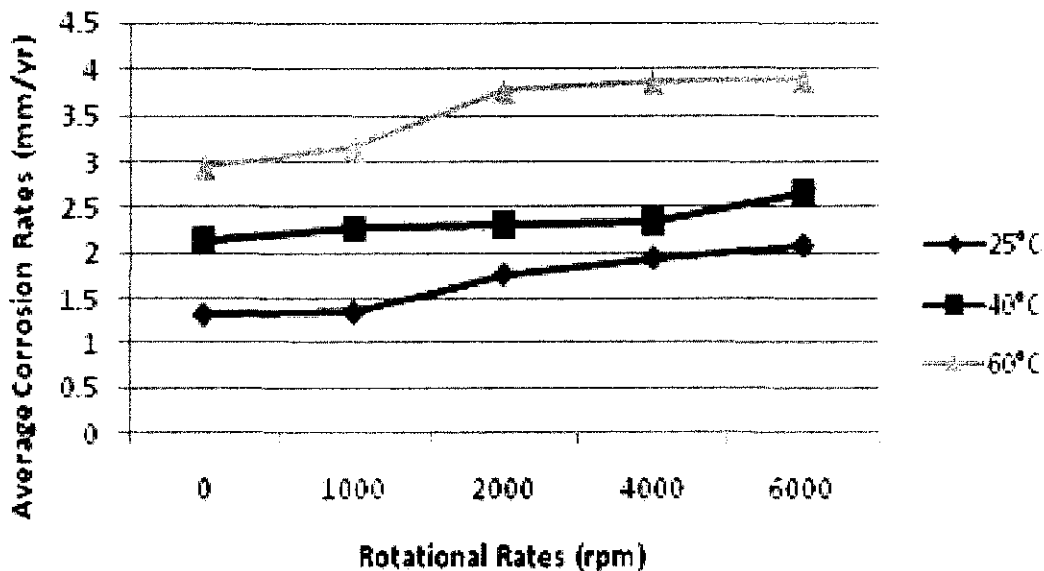


Figure 4.3: Average CO₂ Corrosion Rates from LPR Test at Different Rotational Rates and Different Temperature

4.3.1 Linear Polarization Resistance Method Test: Discussion

The API L-80 steel corrosion rate yields from the experiment are in the range of 1.3 to 3.9 mm/year. At low temperature (25 °C to 40 °C) and rotational rates = 0 rpm, the corrosion rate of samples shows a significant increasing trend from 1.35 mm/yr to 2.26 mm/yr. This is due to the continuous dissolution of Fe²⁺ ions as a result of formation of porous FeCO₃, which is not protective in nature. However, as the temperature increases from 40 °C to 60 °C, the FeCO₃ layer become less porous, more adherent to the L 80 steel surface and protective in nature. Hence, the corrosion rates only increase from 2.26 to 2.90 mm/yr. At higher temperature (above 60 °C), the FeCO₃ is more stable thus protecting the surface from corrosion.

The corrosion rate is increasing significantly when the rotational speed was introduced to the specimens. This is due to the formation of FeCO₃ protective layers were washed away by the fluid velocity. The effect can be seen more clearly at the low temperature (25 °C) experiment where the FeCO₃ layer is more porous. The corrosion rates increased from 1.75 mm/yr at 1000 rpm rotational rates to 2.14 mm/yr at 6000 rpm rotational rates.

The average corrosion rates yield from LPR test is higher than the average corrosion rates yield from Weight Loss Method test. This is due to the short period of LPR test since the corrosion rates were monitored on-time and the data was taken on every 5 minutes intervals for 15 readings. During these 75 minutes, the CO₂ corrosion rate of the L-80 is increasing significantly. However, as the time passed, the corrosion rate is still increasing but at a slower trend due to the formation of FeCO₃ protective layer on the surface. Figure 4.4 shows the typical CO₂ corrosion rates trend in aqueous solution.

For the Weight Loss Method, the test was conducted for 48 hours. Thus, the average CO₂ corrosion rates yield from the test is lower than LPR test due to the protective FeCO₃ layer formed on the specimen surface.

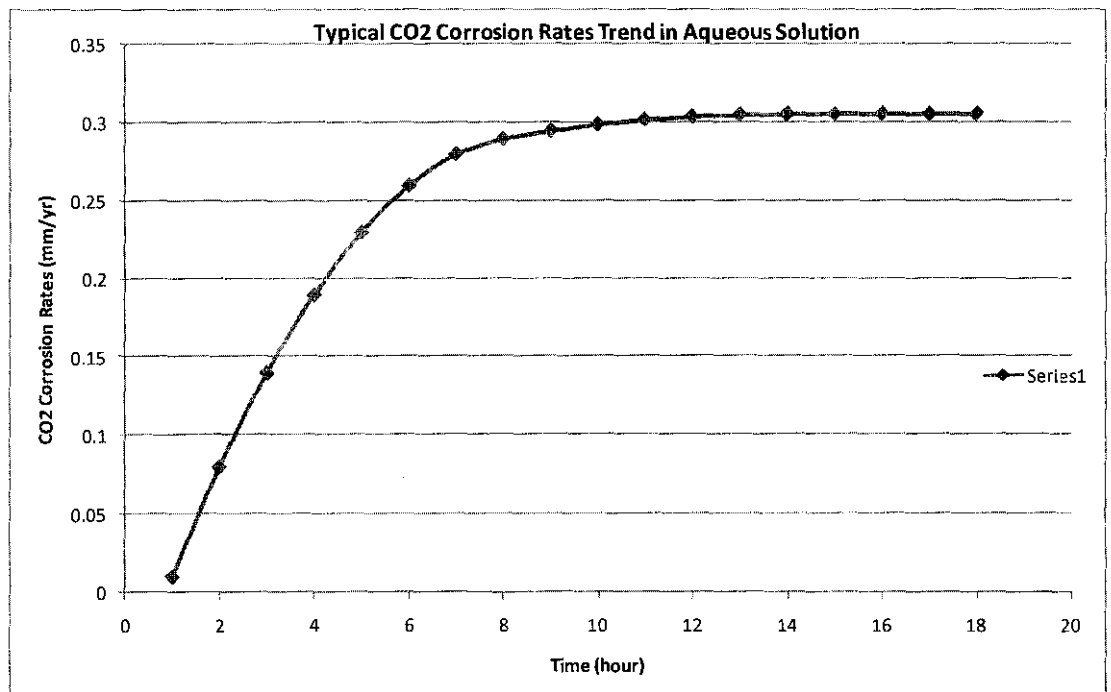


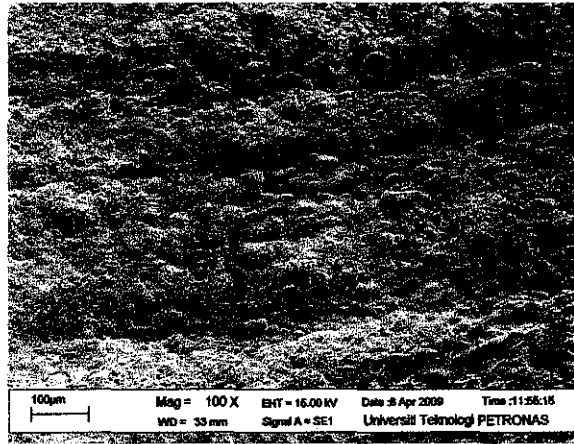
Figure 4.4: Typical CO₂ Corrosion Rates Trend in Aqueous Solution

4.4 Scanning Electron Microscopic Tests Results

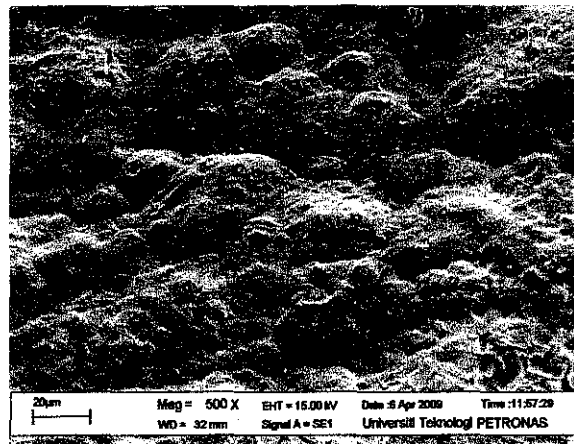
All the specimens were taken to SEM Laboratory after the Weight Loss Method Tests. The test was conducted to understand the micro level aspect of the CO₂ corrosion product in API L-80 steel specimen before and after corroded. The image shows the CO₂ corrosion product and the formation of FeCO₃ layer on the L 80 steel surface. The SEM Tests were conducted on four different L-80 steel specimens:

- a. SEM image of the initial L-80 steel that not-affected with any electrochemical reaction in different magnification
- b. SEM image of L-80 steel immersed for 48 hours in CO₂ saturated 3% NaCl solution at pressure 10 bar and temperature of 25°C in different magnification
- c. SEM image of L-80 steel immersed for 48 hours in CO₂ saturated 3% NaCl solution at pressure 40 bar and temperature of 25°C in different magnification
- d. SEM image of L 80 steel immersed for 48 hours in CO₂ saturated 3% NaCl solution at pressure 60 bar and temperature of 25°C in different magnification

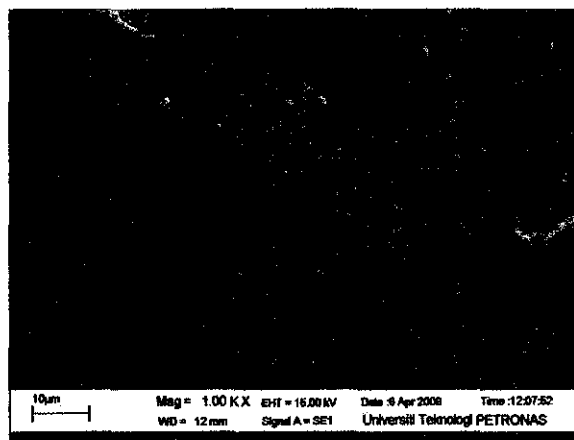
4.4.1 API L-80 Steel



(a)



(b)

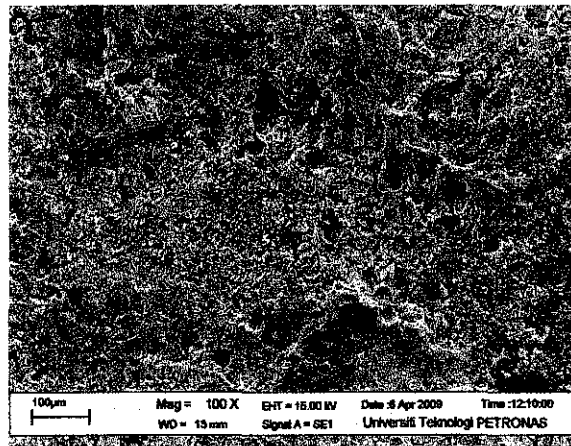


(c)

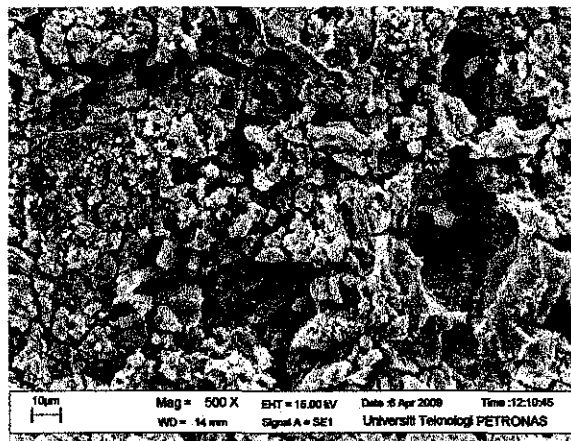
Figure 4.5: SEM micrographs of L-80 steel that not-affected with any electrochemical reaction. (a) 100x (b) 500x (c) 1000x

The SEM micrographs above show the initial surface condition of API L-80 steel specimen before being tested in CO₂ corrosion environment. The surface was fairly smooth without any sign of holes, crack or corrosion products.

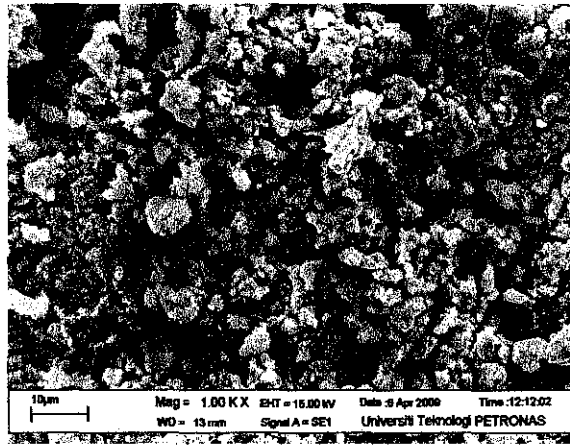
4.4.2 API L-80 Steel after 48 hours immersed in 3% NaCl solutions pH 5, at pressure 10 bar and temperature 25°C.



(a)



(b)

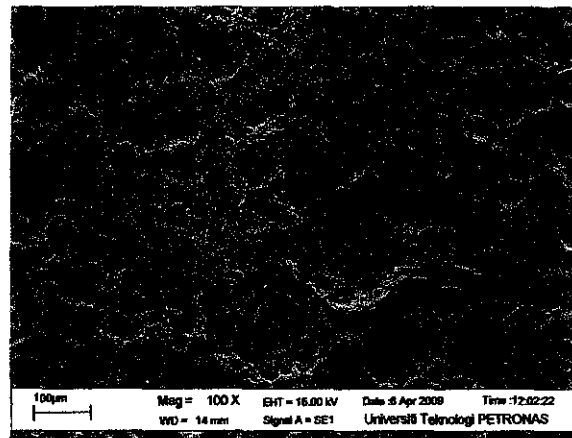


(c)

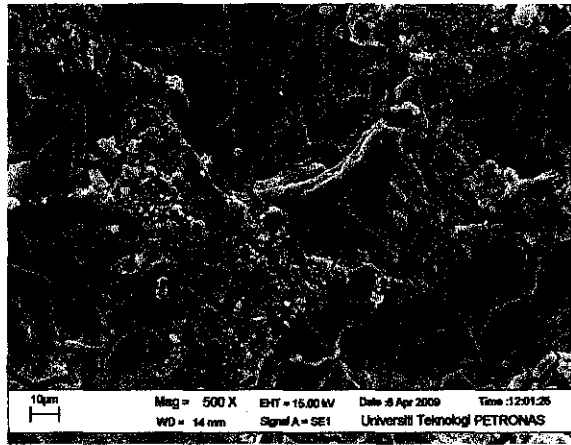
Figure 4.6: L-80 steel specimen at 48 hours immersion in 3% NaCl solution pH=5, at pressure of 10 bar and temperature 25 °C (a) 100x (b) 500x (c) 1000x

The SEM images show the corrosion products, FeCO_3 film layers formed were porous due to the fact that the experiment was conducted at low temperature (25 °C).

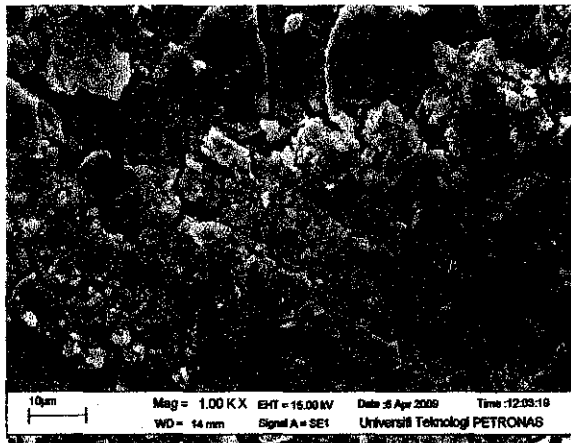
4.4.3 API L-80 Steel after 48 hours immersed in 3% NaCl solutions pH 5, at pressure 40 bar and temperature 25°C.



(a)



(b)

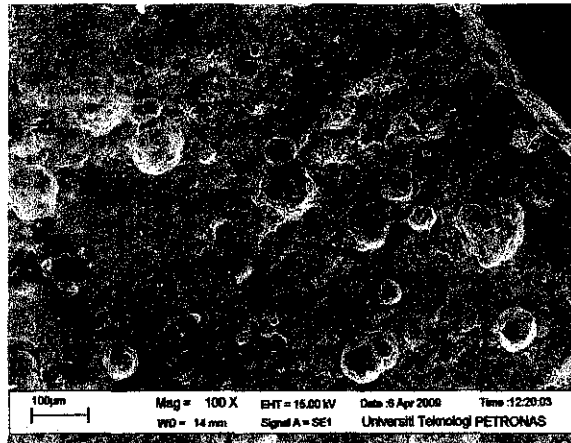


(c)

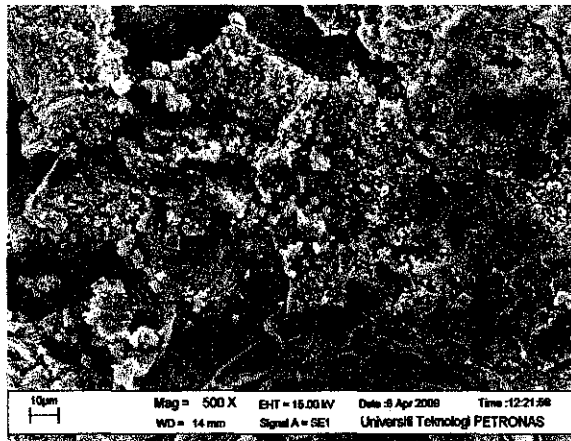
Figure 4.7: L-80 steel specimen at 48 hours immersion in 3% NaCl solution pH=5, at pressure of 40 bar and temperature 25 °C (a) 100x (b) 500x (c) 1000x

The SEM images show the corrosion products, FeCO_3 film layers formed were porous due to the fact that the experiment was conducted at low temperature (25 °C). Some cracks and pitting were identified on the surface due to the high pressure (40 bar) environment used during the test.

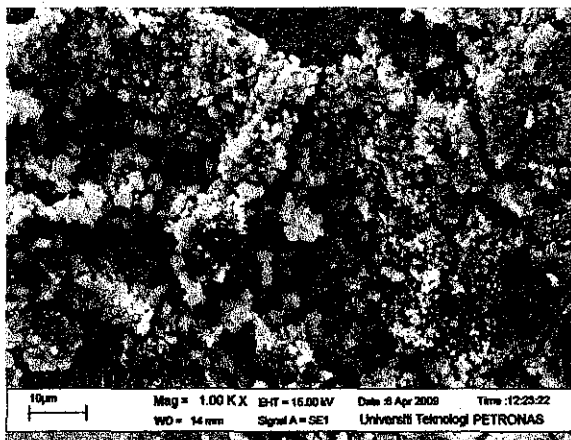
4.4.4 API L-80 Steel after 48 hours immersed in 3% NaCl solutions pH 5, at pressure 60 bar and temperature 25°C.



(a)



(b)



(c)

Figure 4.8: L-80 steel specimen at 48 hours immersion in 3% NaCl solution pH=5, at pressure of 60 bar and temperature 25 °C (a) 100x (b) 500x (c) 1000x

The SEM images show the corrosion products, FeCO_3 film layers formed were porous due to the fact that the experiment was conducted at low temperature (25 °C). The cracks and pitting occurrence on the surface was higher than previous tests due to the higher pressure (60 bar) environment used during the test.

4.5 Optical Microscopic Test Results

The Optical Microscope Test was conducted to understand the surface condition of the specimens. The OM Tests were conducted on four different L-80 steel specimens:

- a. OM image of the initial L-80 steel that not-affected with any electrochemical reaction.
- b. OM image of L-80 steel immersed for 48 hours in CO_2 saturated 3% NaCl solution at pressure 10 bar and temperature of 25°C
- c. OM image of L-80 steel immersed for 48 hours in CO_2 saturated 3% NaCl solution at pressure 40 bar and temperature of 25°C
- d. OM image of L 80 steel immersed for 48 hours in CO_2 saturated 3% NaCl solution at pressure 60 bar and temperature of 25°C

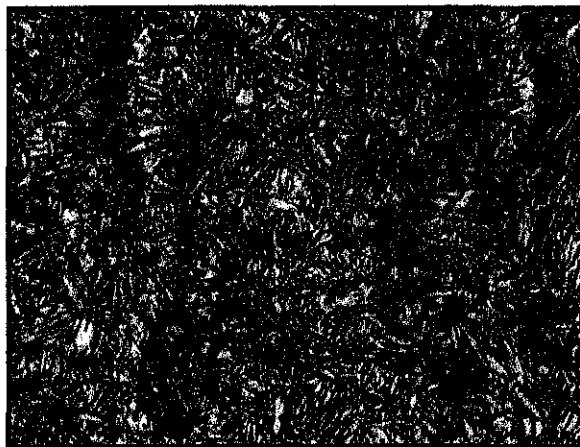


Figure 4.9: OM micrographs of L-80 steel that not-affected with any electrochemical reaction

The OM image above shows the initial surface condition of API L-80 steel specimen before being tested in CO₂ corrosion environment. The surface condition of L-80 steel specimen was smooth and free from any corrosion product.



Figure 4.10: L-80 steel specimen at 48 hours immersion in 3% NaCl solution pH 5, at pressure of 10 bar and temperature 25 °C



Figure 4.11: L-80 steel specimen at 48 hours immersion in 3% NaCl solution pH 5, at pressure of 40 bar and temperature 25 °C

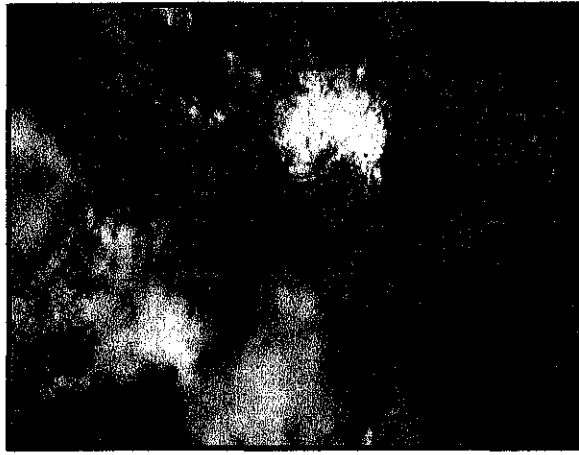


Figure 4.12: L-80 steel specimen at 48 hours immersion in 3% NaCl solution pH 5, at pressure of 60 bar and temperature 25 °C

Figure 4.10, 4.11 and 4.12 show that the corrosion product, FeCO_3 film layers formed on the surface of the L-80 steel specimen. The surface condition was rough, due to the existence of the corrosion products.

4.6 Microhardness (Vicker) Tests Results

Hardness covers several properties such as resistance to deformation, resistance to friction and abrasion which is important parameters for tubing failure. Vicker Hardness Test was conducted to compare the L-80 steel's hardness before and after corrosion using Test Load = 50 gf and Dwell Time = 15 seconds. The hardness average (in Hardness Vicker, HV) is shown in Table 4.5 below. 15 tests were conducted on each specimen:

- a. L-80 steel that not-affected with any electrochemical reaction.
- b. L-80 steel immersed for 48 hours in CO_2 saturated 3% NaCl solution at pressure 10 bar and temperature of 25°C
- c. L-80 steel immersed for 48 hours in CO_2 saturated 3% NaCl solution at pressure 40 bar and temperature of 25°C
- d. L 80 steel immersed for 48 hours in CO_2 saturated 3% NaCl solution at pressure 60 bar and temperature of 25°C

Table 4.5: Average Hardness of L-80 Steel Specimens

No. of Test	Hardness Vicker (HV)			
	Non Corroded L 80 steel	* 10 bar	* 40 bar	* 60 bar
1	984.4	914.6	907.6	947.9
2	973.4	893.4	933.6	900.4
3	835.4	895.8	833.5	874.0
4	916.2	911.2	904.8	960.5
5	958.6	938.2	921.9	966.4
6	958.6	928.6	915.9	922.6
7	849.1	841.1	917.7	970.4
8	914.4	898.7	829.2	986.9
9	953.7	950.9	941.5	948.7
10	924.4	914.9	919.3	877.4
11	970.4	975.4	955.5	870.5
12	868.9	855.9	977.3	928.1
13	993.6	989.3	965.3	892.9
14	958.6	940.8	938.5	904.6
15	951.8	955.2	932.1	855.6
Average	934.10	920.27	919.58	920.46

* L 80 steel immersed for 48 hours in CO₂ saturated 3% NaCl solution at temperature of 25°C

4.6.1 Microhardness (Vicker) Test: Discussion

From the test, the L-80 steel that was not affected with any electrochemical reaction yields average hardness = 934.10 HV. It can be seen that the average hardness of the corroded L-80 steel specimens are not much different with the L-80 specimen in the pressure of 10 bar environment yields average hardness = 920.27 HV, the L-80 specimen in the pressure of 40 bar environment yields average hardness = 919.58 HV and the L-80 specimen in the pressure of 60 bar environment yields average hardness = 920.46 HV.

Based on the theory, electrochemical reaction will not affect the hardness of a material. The test was conducted to prove the theory accuracy with the API L-80 steel material in CO₂ corrosion environment.

From the results obtained, the initial average hardness of L-80 steel was 934.10 HV and the average hardness of corroded L-80 steel was in the range of 919.5 to 920.5 HV. The reason of the decreased value of the L-80 steel average hardness was due to the grinding process that was performed on the specimens to acquire flat surface for the microhardness test to be done.

CHAPTER 5

CONCLUSION AND RECOMMENDATIONS

5.1 Conclusion

In this project, two (2) different tests were performed to measure the CO₂ corrosion rates in API L-80 steel. The following conclusions could be drawn from the study:

- a. The main concern of CO₂ corrosion problem in oil producing well was on the production tubing surface. The other well components such as wellhead, casing and packer were not exposed to the CO₂ corrosion environment during the production. API L-80 steel was the material used in the construction of production tubing.
- b. From the Weight Loss Method using Autoclave Tests results, it showed that the corrosion rates increased slowly from low to high pressure (10 bar, 40 bar and 60 bar). The corrosion rate increased due to local depletion of HCO₃⁻ ions which was favoring the cathodic reaction. The highest corrosion rate yields was at 0.4681 mm/yr (environment; 3 wt% NaCl solution, pressure at 60 bar, pH = 5 and at room temperature).
- c. The LPR results showed that at low temperatures (25°C, 40°C and 60°C), the corrosion rate increased as the temperature increased because of high solubility of the FeCO₃ film layers. However, at temperature of 80°C, for both environments, the FeCO₃ film layers might have become more adherent to the steel surface and more protective in nature resulting in a decrease of the corrosion rate. The highest average corrosion rate obtained was 3.9 mm/yr which was considerably high for the tubing application in oil and gas industry.
- d. In conclusion for both experiments, the CO₂ corrosion rates in high pressure condition were found in the range of 0.23 mm/yr to 0.47 mm/yr and the CO₂ corrosion rates in high temperature condition were in the range of 1.3 to 3.9 mm/yr. Thus, the CO₂ corrosion rates in high temperature and high pressure condition of oil producing well may varied from 0.23 to 3.9 mm/yr.
- e. In order to ensure cost-effective and safe design of production facilities used in the oil and gas industry e.g. oil production tubing well made from L-80

steel, some methods of prevention were identified to be practically used in the field. 1) The usage of adsorption inhibitor such as amine, amide and imidazoline may enhance the formation of FeCO_3 protective layer on the surface of production tubing thus, reduce the CO_2 corrosion rates. 2) Due to the high CO_2 corrosion rate yields from the tests using L-80 steel specimens, other material that has more corrosion resistance than L-80 steel may be considered to be used in the construction of production tubing. For example, the addition of 13% of chromium in the L-80 steel may increase the steel's resistance to corrosive environment. It is also recommended to use 3L epoxy layer on the steel surface will act as a coating and provide protective layer against CO_2 corrosion.

5.2 Recommendations

There are several recommendations that can be performed in future to improve the results of the study:

- a. In determining the realistic results, comparison should be made between the experimental results and the calculation using CO_2 corrosion prediction models such as Cassandra and Norsok to verify the reliability and consistency of the results obtained from laboratory experiment.
- b. Include the pressure and temperature in one experiment to simulate the actual condition of oil producing well using L 80 steel. The values of the temperatures should be increased up to 120°C and the value of pressure should be increased up to 100 bar. This is because under certain conditions, a difference of 5°C and 5 bar can lead to two different corrosion outcomes.
- c. It is known that pH has a strong influence on the CO_2 corrosion rates where it involves in the formation of FeCO_3 film layers. Higher pH resulted in faster formation of more protective films and therefore, various pH such as pH 6.3 and pH 6.6 should be included in future work.
- d. Variation of CO_2 concentration on corrosion rates should be investigated. CO_2 corrosion rate normally is determined by CO_2 partial pressure which is dependent on the system total pressure and CO_2 concentration.

REFERENCES

- [1] Kermani, M. B. and Smith, L. M., *CO₂ Corrosion Control in Oil and Gas Production Design Considerations*, Number 23, London, The Institute of Materials, 1997
- [2] Dr A K Samant, *Oil and Gas Corporation Technical Paper*, India, 2003
- [3] Grigorescu R., *Schlumberger, ROLL Module*, Romania, 2007
- [4] Chaoyang Fu., 2001, *Application of grey relational analysis for corrosion failure of oil tubes*, Corrosion Science 2001
- [5] G. Ramona, *Baker Hughes, Oilfield Familiarization*, Houston, USA, 2006
- [6] Grigorescu R., *Schlumberger, Production Chemistry*, Romania, 2007
- [7] ASTM Committee G01, 2004. *Standard Terminology Relating to Corrosion and Corrosion Testing*. G 15 – 04, ASTM International, United States.
- [8] Stern, M., *Corrosion 1*, Newnes- Butterworths, 1976
- [9] Stern, M., *Corrosion 2: Corrosion Control*, Newnes –Butterworths, 1976
20:35-20:40
- [10] Pourbaix, M., *Electrochemical Corrosion*, 1973
- [11] Mansfeld, F., J., *Journal of the Electrochemical. Society*, 1973
- [12] R. Baboian., *Corosion Test and Standards: Application and Interpretation* (1995), Philadelphia 307-315

- [13] Dean, S. W. Jr., *Corrosion Testing: Encyclopedia of Materials Science and Engineering*, M. B. Ed., Pergamon Press, 1986
- [14] Stern, M. and Weisert, E. D., *Experimental Observations on the Relation between Polarization Resistance and Corrosion Rate*, in *ASTM Proceedings*, Vol. 59, American Society for Testing and Materials, Philadelphia, 1959, p. 1280
- [15] *Corrosion Control in Petroleum Production*, National Association of Corrosion Engineering, 1979, Houston
- [16] M. Stern and A.L. Geary, *Electrochemical Polarization*, *Journal of the Electrochemical Society*, Vol. 104, No.1, 1957, p.56
- [17] ASTM Committee G01, 2004. *Standard Practice for Laboratory Immersion Corrosion Testing of Metals*. G 31 – 72, ASTM International, United States.
- [18] ASTM Committee G01, 2003. *Standard Test Method for Conducting Potentiodynamic Polarization Resistance Measurements* G 59 – 97, ASTM International, United States.

APPENDICES



Standard Test Method for Conducting Potentiodynamic Polarization Resistance Measurements¹

This standard is issued under the fixed designation G 59; the number immediately following the designation indicates the year of original adoption or, in the case of revision, the year of last revision. A number in parentheses indicates the year of last reapproval. A superscript epsilon (ϵ) indicates an editorial change since the last revision or reapproval.

1. Scope

1.1 This test method describes an experimental procedure for polarization resistance measurements which can be used for the calibration of equipment and verification of experimental technique. The test method can provide reproducible corrosion potentials and potentiodynamic polarization resistance measurements.

1.2 *This test method does not purport to address all of the safety concerns, if any, associated with its use. It is the responsibility of the user of this standard to establish appropriate safety and health practices and determine the applicability of regulatory limitations prior to use.*

2. Referenced Documents

2.1 ASTM Standards:

G 3 Practice for Conventions Applicable to Electrochemical Measurements in Corrosion Testing²

G 5 Test Method for Making Potentiostatic and Potentiodynamic Anodic Polarization Measurements²

G 102 Practice for Calculation of Corrosion Rates and Related Information from Electrochemical Measurements²

2.2 Adjunct:

Samples of the Standard AISI Type 430 Stainless Steel (UNS S43000)³

3. Significance and Use

3.1 This test method can be utilized to verify the performance of polarization resistance measurement equipment including reference electrodes, electrochemical cells, potentiostats, scan generators, measuring and recording devices. The test method is also useful for training operators in sample preparation and experimental techniques for polarization resistance measurements.

3.2 Polarization resistance can be related to the rate of general corrosion for metals at or near their corrosion potential, i_{corr} . Polarization resistance measurements are an accurate and

rapid way to measure the general corrosion rate. Real time corrosion monitoring is a common application. The technique can also be used as a way to rank alloys, inhibitors, and so forth in order of resistance to general corrosion.

3.3 In this test method, a small potential scan, $\Delta E(t)$, defined with respect to the corrosion potential ($\Delta E = E - E_{corr}$), is applied to a metal sample. The resultant currents are recorded. The polarization resistance, R_p , of a corroding electrode is defined from Eq 1 as the slope of a potential versus current density plot at $i = 0$ (1-4):⁴

$$R_p = \left(\frac{\partial \Delta E}{\partial i} \right)_{i=0, \partial E/\partial t \rightarrow 0} \quad (1)$$

The current density is given by i . The corrosion current density, i_{corr} , is related to the polarization resistance by the Stern-Geary coefficient, B . (3),

$$i_{corr} = 10^6 \frac{B}{R_p} \quad (2)$$

The dimension of R_p is ohm-cm², i_{corr} is $\mu\text{A}/\text{cm}^2$, and B is in V. The Stern-Geary coefficient is related to the anodic, b_a , and cathodic, b_c , Tafel slopes as per Eq 3.

$$B = \frac{b_a b_c}{2.303(b_a + b_c)} \quad (3)$$

The units of the Tafel slopes are V. The corrosion rate, CR , in mm per year can be determined from Eq 4 in which EW is the equivalent weight of the corroding species in grams and ρ is the density of the corroding material in g/cm³.

$$CR = 3.27 \times 10^{-3} \frac{i_{corr} EW}{\rho} \quad (4)$$

Refer to Practice G 102 for derivations of the above equations and methods for estimating Tafel slopes.

3.4 The test method may not be appropriate to measure polarization resistance on all materials or in all environments. See 8.2 for a discussion of method biases arising from solution resistance and electrode capacitance.

4. Apparatus

4.1 The apparatus is described in Test Method G 5. It includes a 1 L round bottom flask modified to permit the

¹ This practice is under the jurisdiction of ASTM Committee G01 on Corrosion of Metals, and is the direct responsibility of Subcommittee G 01.11 on Electrochemical Measurements in Corrosion Testing.

Current edition approved Dec. 10, 1997. Published February 1998. Originally approved in 1978. Last previous edition approved in 1991 as G 59 – 91.

² *Annual Book of ASTM Standards*, Vol 03.02.

³ Available from ASTM Headquarters. Order PCN 12-700050-00.

⁴ The boldface numbers in parentheses refer to the list of references at the end of this standard.

addition of inert gas, thermometer, and electrodes. This standard cell or an equivalent cell can be used. An equivalent cell must be constructed of inert materials and be able to reproduce the standard curve in Test Method G 5.

4.2 A potentiostat capable of varying potential at a constant scan rate and measuring the current is needed.

4.3 A method of recording the varying potential and resulting current is needed.

Test of Electrical Equipment

5.1 Before the polarization resistance measurement is made, the instrument system (potentiostat, X-Y recorder or data acquisition system) must be tested to ensure proper functioning. For this purpose, connect the potentiostat to a test electrical circuit (5). While more complex dummy cells are sometimes needed in electrochemical studies, the simple resistor shown in Fig. 1 is adequate for the present application.

5.2 Use $R = 10.0 \Omega$. Set the applied potential on the potentiostat to $E = -30.0$ mV and apply the potential. The current should be 3.0 mA by Ohm's Law, $I = E/R$.

NOTE 1—When polarization resistance values are measured for systems with different corrosion currents, the value of R should be chosen to cover the current range of the actual polarization resistance measurement. Expected corrosion currents in the microampere range require $R = 1$ to 10Ω .

5.3 Record the potentiodynamic polarization curve at a scan rate of 0.6 V/h from $\Delta E = -30$ mV to $\Delta E = +30$ mV and back to $\Delta E = -30$ mV. The plot should be linear, go through the origin, and have a slope 10Ω . The curves recorded for the forward and reverse scans should be identical.

5.4 If the observed results are different than expected, the electrochemical equipment may require calibration or servicing in accordance with the manufacturer's guidelines.

Experimental Procedure

6.1 The 1.0 N H_2SO_4 test solution should be prepared from American Chemical Society reagent grade acid and distilled water as described in Test Method G 5. The standard test cell requires 900 mL of test solution. The temperature must be maintained at 30°C within 1°.

6.2 The test cell is purged at 150 cm³/min with an oxygen-free gas such as hydrogen, nitrogen, or argon. The purge is continued at least 30 min before specimen immersion. The purge continues throughout the test.

6.3 The working electrode should be prepared as detailed in Test Method G 5. The experiment must commence within 1 h of preparing the electrode. Preparation includes sequential wet polishing with 240 grit and 600 grit SiC paper. Determine the

surface area of the specimen to the nearest 0.01 cm² and subtract for the area under the gasket (typically 0.20 to 0.25 cm²).

6.4 Immediately prior to immersion the specimen is degreased with a solvent such as acetone and rinsed with distilled water. The time delay between rinsing and immersion should be minimal.

NOTE 2—Samples of the standard AISI Type 430 stainless steel (UNS S45000) used in this test method are available to those wishing to evaluate their equipment and test procedure from Metal Samples, P.O. Box 8, Mumford, AL 36268.

6.5 Transfer the test specimen to the test cell and position the Luggin probe tip 2 to 3 mm from the test electrode surface. The tip diameter must be no greater than 1 mm.

6.6 Record the corrosion potential E_{corr} after 5 and 55-min immersion.

6.7 Apply a potential 30 mV more negative than the recorded 55 min corrosion potential (See Note 3).

NOTE 3—Practice G 3 provides a definition of sign convention for potential and current.

6.8 One minute after application of the -30 mV potential, begin the anodic potential scan at a sweep rate of 0.6 V/h (within 5%). Record the potential and current continuously. Terminate the sweep at a potential 30 mV more positive than the 55 min corrosion potential.

6.9 Plot the polarization curve as a linear potential-current density plot as shown in Practice G 3. Determine the polarization resistance, R_p , as the tangent of the curve at $i=0$.

7. Report

7.1 Report the following information:

7.1.1 The 5 and 55 min corrosion potentials and the polarization resistance value,

7.1.2 Duplicate runs may be averaged, and

7.1.3 Note any deviation from the procedure or test conditions established in this test method.

8. Precision and Bias

8.1 Precision—Precision in this test method refers to the closeness of agreement between randomly selected measured values. There are two aspects of precision, repeatability and reproducibility. Repeatability refers to the closeness of agreement between measurements by the same laboratory on identical Type 430 stainless steel specimens repeated with as close as possible adherence to the same procedure. Reproducibility refers to the closeness of agreement between different laboratories using identical Type 430 stainless steel specimens and

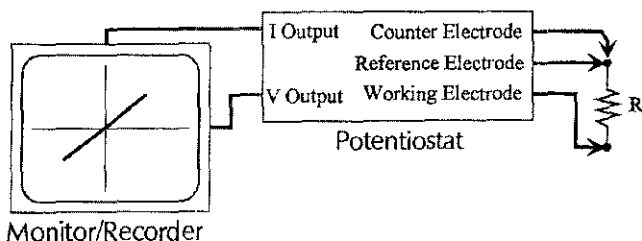


FIG. 1 Arrangement for Testing of Electrical Equipment (Potentiostat, X-Y Recorder)

the procedure specified. An interlaboratory test program with 13 laboratories participating and two, three or four replicate measurements was carried out to establish the precision. The measured values included (Table 1) the corrosion potential measured after 5 and 55 min and the polarization resistance. A research report has been filed with the results of this program.

8.1.1 *Repeatability*—The lack of repeatability is measured by the repeatability standard deviation s_r . The 95 % confidence interval was calculated as $\pm 2.8 s_r$. The values obtained are shown in Table 2. The 95 % confidence interval refers to the interval around the average that 95 % of the values should be found.

TABLE 1 Interlaboratory Test Program Polarization Data for Stainless Steel Type 430 in 1.0 N H₂SO₄ at 30°C

Laboratory	E_{corr} -5min (mV)	E_{corr} -55min (mV)	R_p (ohm-cm ²)
1	-0.519	-0.506	6.47
	-0.519	-0.505	5.88
2	-0.542	-0.521	5.95
	-0.540	-0.519	5.04
3	-0.524	-0.513	6.93
	-0.520	-0.508	6.40
4	-0.555	-0.545	7.70
	-0.565	-0.545	7.70
5	-0.539	-0.524	7.58
	-0.530	-0.510	6.18
6	-0.519	-0.510	7.60
	-0.522	-0.512	7.16
	-0.521	-0.509	6.65
7	-0.522	-0.510	9.06
	-0.520	-0.511	7.07
	-0.523	-0.510	5.85
8	-0.520	-0.508	7.11
	-0.520	-0.508	7.52
	-0.521	-0.510	6.94
9	-0.529	-0.513	7.11
	-0.530	-0.513	7.22
	-0.529	-0.514	7.19
	-0.529	-0.515	7.19
10	-0.514	-0.505	5.17
	-0.516	-0.506	6.90
11	-0.543	-0.529	5.07
	-0.538	-0.524	4.64
12	-0.520	-0.505	5.63
	-0.519	-0.507	6.16
13	-0.531	-0.519	5.08
	-0.529	-0.517	5.38
	-0.529	-0.517	5.90

TABLE 2 Repeatability Statistics

	Average	S_r	95 % Confidence Interval
E_{corr} , 5 min, mV versus SCE	-0.5287	0.00260	± 0.0073 V
E_{corr} , 55 min, mV versus SCE	-0.5151	0.00273	± 0.0076 V
R_p , ohm-cm ²	6.46	0.713	± 2.00 ohm-cm ²

8.1.2 *Reproducibility*—The lack of reproducibility is measured by the reproducibility standard deviation, s_R . The 95 % confidence interval was calculated as $\pm 2.8 s_R$. The values obtained are shown in Table 3.

TABLE 3 Reproducibility Statistics

	Average	S_R	95 % Confidence Interval
E_{corr} , 5 min, mV versus SCE	-0.5287	0.0127	± 0.0356 mV
E_{corr} , 55 min, mV versus SCE	-0.5151	0.0111	± 0.0311 mV
R_p , ohm-cm ²	6.46	1.01	± 2.83 ohm-cm ²

8.2 *Bias*—The polarization resistance as measured by the Test Method G 59 has two sources of bias. The potentiodynamic method includes a double layer capacitance charging effect that may cause the polarization resistance to be underestimated. There is also a solution resistance effect that may cause the polarization resistance to be overestimated. This bias will depend on the placement of the reference electrode and electrolyte conductivity. Refer to Practice G 102 for further discussion on the effects of double layer capacitance and solution resistance on polarization resistance measurements.

9. Keywords

9.1 anodic polarization; auxiliary electrode; cathodic polarization; corrosion; corrosion potential; corrosion rate; current density; electrochemical cell; electrochemical potential; Luggin probe; mixed potential; open-circuit potential; overvoltage; polarization resistance; potentiodynamic; reference electrode; solution resistance; Stern-Geary coefficient; Tafel slope; working electrode

REFERENCES

- 1) Stern, M., and Roth, R. M., *Journal of the Electrochemical Society*, Vol 104, 1957, p. 390.
- 2) Stern, M., *Corrosion*, Vol 14, 1958, p. 440 t.
- 3) Mansfeld, F., "The Polarization Resistance Technique for Measuring Corrosion Currents", *Corrosion Science and Technology*, Plenum Press, New York, NY, Vol VI, 1976, p.163.
- 4) Mansfeld, F., "Evaluation of Polarization Resistance Round Robin Testing Conducted by ASTM G01.11", Paper No. 106, CORROSION/76, NACE, Houston, TX, March 22-26, 1976.
- 5) Gileadi, E., Kirowa-Eisner, E., and Penciner, J. *Interfacial Electrochemistry, an Experimental Approach*, Chapter III.1, Addison-Wesley Publishing Co., Reading, MA 1975.

 **G 59 – 97 (2003)**

ASTM International takes no position respecting the validity of any patent rights asserted in connection with any item mentioned in this standard. Users of this standard are expressly advised that determination of the validity of any such patent rights, and the risk of infringement of such rights, are entirely their own responsibility.

This standard is subject to revision at any time by the responsible technical committee and must be reviewed every five years and if not revised, either reapproved or withdrawn. Your comments are invited either for revision of this standard or for additional standards and should be addressed to ASTM International Headquarters. Your comments will receive careful consideration at a meeting of the responsible technical committee, which you may attend. If you feel that your comments have not received a fair hearing you should make your views known to the ASTM Committee on Standards, at the address shown below.

This standard is copyrighted by ASTM International, 100 Barr Harbor Drive, PO Box C700, West Conshohocken, PA 19428-2959, United States. Individual reprints (single or multiple copies) of this standard may be obtained by contacting ASTM at the above address or at 610-832-9585 (phone), 610-832-9555 (fax), or service@astm.org (e-mail); or through the ASTM website (www.astm.org).